Origin and geochemistry of arsenic in surface and groundwaters of Los Pozuelos basin, Puna region, Central Andes, Argentina

Jesica Murray, D. Kirk Nordstrom, Bernhard Dold, Maria Romero Orué, Alicia Kirschbaum

Origin and geochemistry of arsenic in surface and groundwaters of Los Pozuelos basin, Puna region, Central Andes, Argentina

Jesica Murray [1,2*]; D. Kirk Nordstrom [3]; Bernhard Dold [4]; Maria Romero Orué [1]; Alicia Kirschbaum[1]

[1]*Instituto de Bio y Geo Ciencias del Noroeste Argentino, Universidad Nacional de Salta - CONICET, 4405 Rosario de Lerma, Argentina.*

[2]*Laboratoire d'Hydrologie et de Géochimie de Strasbourg, Université de Strasbourg, EOST, CNRS, 67084 Strasbourg, France*

[3]*United States Geological Survey, Boulder, CO, 80303 United States of America*

[4]*Division of Geosciences and Environmental engineering, Luleå University of Technology, 971 87 Luleå, Sweden*

*Corresponding author: Dr. Jesica M. Murray

murray.jesica@gmail.com

Postal Address: 9 de Julio, 14, Rosario de Lerma, (CP 4405), Argentina.

Abstract

Los Pozuelos is a closed basin in the Puna region of NW Argentina, Central Andes. This is a semi-arid region where closed basins are the most important feature for the hydrologic systems. The center of the basin is occupied by a fluctuating playa lake called Los Pozuelos lagoon, which constitutes a UNESCO Biosphere Reserve. This is one of the most populated closed basins in the Argentinian Puna and residents use groundwater for drinking and cooking. Lowest concentrations of As and dissolved solids are in the headwaters of the rivers (1.46 – 27 µg/L) and

the highest concentrations are in the lagoon (43.7 - 200.3 µg/L). In groundwater, arsenic concentrations increase from the outer ring aquifer (3.82 - 29.7 µg/L) composed of alluvial-alluvial fan sediments to the inner lacustrine aquifer (10 - 113 µg/L) that surround the playa lake. Moreover, high concentrations of As during the dry season (90.2 and 113 µg/L), Na/K mass ratios (0.2 and 0.3), and formation of Na-rich efflorescent salts suggest that high evaporation rates increases As concentration, while rainwater dilutes the concentration during the wet season. As (V) is the dominant species in all the water types, except for the lagoon, where As(III) occasionally dominates because of organic matter buildup. There are at least three potential sources for As in water i) oxidation of As sulfides in Pan de Azúcar mine wastes, and acid mine drainage discharging into the basin; ii) weathering and erosion of mineralized shales; iii) weathering of volcanic eruptive non-mineralized rocks. Because it is a closed basin, the arsenic released from the natural and anthropogenic sources is transported in solution and in fluvial sediments and finally accumulates in the center of the basin where the concentration in water increases by evaporation with occasional enhancement by organic matter interaction in the lagoon.

Key words: Altiplano-Puna, closed basin, arsenic redox speciation, evaporation, UNESCO Biosphere Reserve

1. Introduction

Argentina was the first Latin American country where arsenic (As) occurrence in groundwater was reported and the first in the world to document As poisoning from natural sources (Bundschuh et al., 2012). Most of the studies in this country have been focused in the Chaco-Pampean plain region, which is known as one of the most extensive areas in the world with high As concentration in surface water and groundwater (Nicolli et al., 2012). However, in the Puna

45 region of NW Argentina, the presence of As in groundwater above the limit for human
46 consumption recommended by the World Health Organization (10 µg/L) was reported and
47 related to the weathering of volcanic rocks (de Sastre et al., 1992, Farias et al., 2009). The Puna
48 region, between 22° and 26° latitude south, forms the south-half portion of the Altiplano-Puna
49 plateau in Central Andes which extends through parts of Argentina, Bolivia, Chile and Peru,
50 between 3,500 and 4,500 m above sea level (see Tapia et al., 2019, this issue). It is the second
51 highest plateau in the Earth after Tibet. Here, the altitude and widening of the Andes produces
52 distinctive meteorological conditions making it a semi-arid region, with high temperatures
53 fluctuations, intense solar irradiation, and high evaporation. More than 70% of the precipitation
54 occurs in the austral summer decreasing westwards and southwards from 700 to <50 mm per
55 year (Garreaud et al., 2003). In this region the Cenozoic volcanism and closed basin hydrology
56 are the most important features. Drainages are not connected to the ocean and terminate in big
57 lakes and salt flats in the center of the basins.

58 High levels of As have been detected in all the types of waters in the Altiplano-Puna (Tapia et
59 al., 2019, this issue). However, only a few publications report arsenic speciation as well as a
60 complete physical-chemical characterization of the waters that help to understand the mobility of
61 arsenic in the closed basins (Tapia et al., 2019, this issue). Extensive studies related to the
62 geogenic and anthropogenic origin of arsenic in the region are also scarce.

63 High concentration of As in urine and hair in woman and children in local Andean communities
64 associated with arsenic-contaminated water were detected (Concha et al., Concha et al., 1998;
65 and 2010), especially in some areas with very high arsenic concentration like San Antonio de
66 Los Cobres. This is an emblematic site situated in the Puna of Argentina where the As
67 consumption in drinking water is ≈ 200 µg/L. Here the arsenic source is associated with acid

68 volcanic eruptive rocks, volcanic ash, and also hydrothermal activity (de Sastre et al., 1992;
69 Farías et al., 2009; Hudson-Edwards and Archer 2012). Recently, Schlebusch et al. (2015)
70 identified the presence of the AS3MT gene in the local aboriginal community of San Antonio de
71 Los Cobres, which have habited the region from more than 10,000 yrs. This is a major gene for
72 arsenic metabolism in humans leading to human adaptation to arsenic-rich environments.

73 Los Pozuelos is one of the most populated closed basins in the Argentinian Puna with a total
74 population of about 3,500 (Cajal, 1998; INDEC, 2010). The local original communities are
75 dispersed along the basin and groundwater is used as drinking and cooking water by most of the
76 inhabitants. Previous studies indicate the presence of arsenic in surface and groundwater of the
77 basin associated to different anthropogenic and geogenic sources (Murray et al., 2016).

78 The aim of this work is to understand the origin of As, its mobility, and cycling in surface and
79 groundwater of Los Pozuelos basin. Arsenic from different anthropogenic and geogenic sources
80 migrate downstream and converge in the center of the closed basin where evaporation may
81 increase its concentration. To achieve our objective we analyzed and interpreted long term data
82 (2011 to 2017) that includes arsenic concentration, arsenic redox speciation, and the
83 geochemistry (major ions and physical-chemical parameters) of surface and groundwaters of the
84 basin. Moreover, the effect of the geomorphological closed hydrologic system and semi-arid
85 conditions on As mobility, concentration, and cycling are discussed. This work contributes to the
86 larger framework of arsenic sources, mobility, and cycling in the closed basins of the Altiplano-
87 Puna.

88 **2. Setting of Los Pozuelos basin**

89 *2.1. Geology*

90 Pozuelos is a closed NNE–SSW piggyback basin located in the Puna morphotectonic province
91 from the Central Andes Altiplano-Puna Plateau (Allmendinger et al., 1997; Rubiolo, 1997).
92 Tectonostratigraphic relationships indicate that Pozuelos basin formed in the late Oligocene –
93 early Miocene between 28 to 16 Ma (Rubiolo, 1997). This basin is bounded by westward-
94 verging thrust sheets. These sheets uplifted Ordovician marine shales (Fm. Acoite) forming the
95 Rinconada Range in the west and Ordivician volcanic-sedimentary rocks (Cochinocha-Escaya
96 Complex) in the east, forming the Cochinoca-Escaya Range (Rubiolo et al., 1997; Caffe et al.,
97 2001) (Fig. 1A). The basin has a surface area of 3800 km^2 (*ca* 110 km long and *ca* 25 km wide),
98 it is located about 3650 m above sea-level and the relief between its bottom and the crests of the
99 marginal mountain ranges exceeds 700 m.

100 The center of this depression is occupied by the Los Pozuelos lagoon, which is a large seasonally
101 fluctuating playa lake (McGlue et al., 2012). The lagoon surface can exceed 135 km^2 during
102 years with above average precipitation (Igarzabal, 1978). The lagoon constitutes one important
103 refuge of aquatic habitat within a desert matrix in Central Andes and harbors protected bird
104 species such as New World Flamingos (*Phoenicopterus jamesi, Phoenicopterus andinus,*
105 *Phoenicopterus chilensis*) (Cendrero et al., 1993; Caziani et al., 2001). Due to its environmental
106 importance the lagoon has been declared a National Natural Monument by the Argentinian
107 government (National Parks Administration of Argentina), Ramsar Site (Ramsar Sites
108 Information Service), and a site of importance for migratory shore birds (Western Hemisphere
109 Shorebird Reserve Network). The whole basin constitutes a UNESCO Biosphere Reserve from
110 1990 (UNESCO Biosphere Reserves).

111 Intervals of prolonged drought commonly lead to desiccation of the playa lake. During this
112 period, the exposure of lacustrine mud and the formation of some salts crust are common, but it

113 does not form a saline deposit such as others in the Altiplano-Puna (Igarzabal, 1978; 1991).
114 Santa Catalina and Cincel Rivers are the most important rivers in the basin with discharges in the
115 lagoon (Igarzabal, 1978). In wet season, the lagoon level shows a rapid recovery of the water
116 surface. When completely filled, the lagoon reaches a maximum depth near its centre (< 2 m)
117 and progressively shoals towards its margins (Igarzabal, 1978; McGlue et al., 2012).

118 The lithology of the basin is diverse in composition and age (Coira and Zappettini, 2008).
119 Ordovician marine shales are the most abundant rocks in the basin and contain many epithermal
120 Au-Pb-Ag-Zn deposits and placer deposits (Rubiolo et al., 1997; Segal and Caffe, 1999; Caffe et
121 al., 2001; Rodriguez et al., 2001; Rodriguez and Bierlein, 2002) (Fig. 1A). Epithermal Au is
122 hosted in small quartz veins, which also are rich in arsenopyrite and pyrite (Segal et al., 1997).
123 The Au mineralization is structurally controlled and occurs typically along large anticline hinges.
124 Geochemical data indicate that the hydrothermal systems are rich in Au-As and Sb together with
125 subordinate quantities of base metals (Pb, Zn, Cu, and Mo; Rodriguez et al., 2001). The
126 exploitation of these Au deposits along the whole Rinconada hill are known from previous
127 colonial times, but are inactive at the present. Cretaceous continental sediments such as
128 sandstones and conglomerates (Pirgua Subgroup) are present in the southern end of the basin
129 (Rubiolo et al., 1997; Caffe et al., 2001) (Fig.1A). Miocene mixed continental sediments
130 including volcanoclastic rocks, sandstones, conglomerates, and carbonates, crop out in the
131 Cochinoca-Escaya Range as well as in the southern end of the basin (Fm. Moreta, Fm. Cara-
132 Cara, Fm. Tiomayo; Rubiolo et al., 1997). Several Miocene dacitic volcanic centers domes
133 (Pozuelos Volcanic Complex) contain Pb-Ag-Zn sulfide mineralized veins that were mined until
134 the nineties (Pan de Azúcar, Cerro Redondo, and Chinchillas mines; Segal and Caffe, 1999).
135 Miocene ignimbrite deposits also comprise some of the epithermal and placer deposits, which are

136 common along the eastern flank and south border of the basin (Coranzulí Complex, Caffe et al.,
137 2001) shown in Fig. 1A. Conglomerates and alluvial fans were deposited at the foot of
138 Rinconada Hills during the Pliocene.

139 In the central area of the basin, Late Pleistocene-Holocene lacustrine deposits surround the actual
140 lagoon as a product of ancient fluctuations of the playa lake (Igarzabal, 1978; Camacho and
141 Kulemeyer 2017). The thickness of these sediments is variable and are composed of silts with
142 minor clay fraction and fine sand with abundant quartz (Igarzabal, 1978). Calcareous levels,
143 gypsum-halite, ostracods, algae, diatoms, and gyttja are present in these sediments (Igarzabal,
144 1978; Camacho and Kulemeyer, 2017). Moreover, efflorescent salts precipitate in the surface as
145 a result of capillary forces induced by strong evaporation (Igarzabal, 1978). The lacustrine
146 sediments intercalate progressively with Pleistocene-Holocene alluvial and alluvial fan deposits
147 situated at the foot of Rinconada and Cochinoca-Escaya hills (Igarzabal, 1978; Camacho and
148 Kulemeyer, 2017). Finally, thin riverbed and floodplain deposits of Cincel and Santa Catalina
149 rivers overly the lacustrine sediments and central parts of the basin occupied by the meandering
150 rivers. They are composed of sand, silt as well as salt precipitation (Igarzabal, 1978; Camacho
151 and Kulemeyer, 2017) (Fig. 1 A).

152 The lacustrine and alluvial-alluvial fan sediments comprise the unconfined aquifer that hosts
153 groundwater in Los Pozuelos basin (Igarzábal, 1978; Alcalde, 2008). Previous studies indicate
154 that the water table is shallow, the piezometric surface is North-South elongated, and the
155 drainage goes to the central area of the basin (Alcalde, 2008).

156 *2.2. Weather and vegetation*

157 Available meteorological data in Los Pozuelos basin from the middle 1970's to middle 1990's
158 can be found in the Instituto Nacional de Tecnologia Agropecuaria (INTA) database (Bianchi

159 and Yañez, 1992). Data from the town of Rinconada, from 1972 to 1996 located in the mid-west
160 area of the basin (Fig. 1) indicates that this is a semi-arid region with an annual precipitation of
161 486 mm occurring mainly in the Austral summer between December and March (Fig. 2). The
162 annual potential evapotranspiration is higher (530 mm) than the annual precipitation and the
163 deficit increases from April to November (Fig. 2). The lowest temperatures occur in winter with
164 a mean value of 1.7 °C for July, while the highest temperatures occur in summer with a mean
165 value of 9.4 °C for January and February.

166 The vegetation of the basin is composed of plant assemblages that generally follow topographic
167 and soil-moisture gradients. The dominant plants are the shrubs *hemicryptophytes* and
168 *nanophanerophytes* (Bonaventura et al., 1995). Some lead-zinc analysis from vegetation sampled
169 at different distances from the Pan de Azúcar mine, indicate that most plants contain zinc in their
170 biomasses as a necessary nutrient, while plants growing closer to the mine contain lead providing
171 evidence of contamination from the mine (Plaza Cazón et al., 2013).

172 **3. Methods**

173 *3.1. Sample collection, preservation, and analysis*

174 *3.1.1. Water samples collection*

175 A total of 120 water samples were obtained from rivers (n = 32), lagoon (n = 6) and groundwater
176 (n = 28), which were sampled during 6 field campaigns between 2011 and 2017 (Table ST1).
177 The sampling design attempted to cover the whole basin from the higher areas to the center of
178 the basin (Fig. 1). In rivers the sampling sites were located at the head waters of the main rivers,
179 at intermediate distances, and at the discharge point in the lagoon. In the lagoon the samples
180 were taking from the North and the South borders. The wells were selected in order to cover the

two different aquifers in the basin, this campaign was mainly possible in the south area of the basin due to higher amount of existing wells. Before sampling, 10 buckets of water from the bottom of the well were taken out, after that, another bucket from the bottom was taken to get the water sample. Only at W9 site it was possible to pump the well for 10 min before taking the sample. Not all the sites were accessible during wet season due to flood conditions, for that reason not only the field campaigns but the number of samples obtained is lower than during the dry season (Table ST1).

Measurements of conductivity, temperature, dissolved oxygen, and pH were performed on site with multi-parametric Hanna equipment (Codes HI991300N and HI9142). All samples were filtered with 0.2 µm pore size HV (Millex) filtration units by using a syringe in some cases and with polyethersulfone (GVS) 0.2 and 0.45 µm membrane filters using a filter holder (Thermo Scientific) and manual pump. The samples were stored in a cooler at 4º C in polyethylene tubes and bottles pre-cleaned with deionized water for anions and 5% HNO_3 for cations, rinsed three times with deionized water after treatment. The samples for cation analyses were acidified to pH < 2 with ultrapure HNO_3 and the samples for anions were only filtered.

3.1.1.1. Major and trace elements analyses

Samples from 2011, 2012, and 2013 periods were analyzed at Actlabs laboratories (Canada). Cations were determined by inductively coupled plasma - optical emission spectrometry (ICP-OES) and by inductively coupled plasma - mass spectrometry (ICP-MS) to obtain the concentration of those elements below detection limits by ICP-OES. Anion concentrations were determined by ion chromatography (IC) at ActLabs laboratories for 2011 and 2012 samples and at University of Brasilia for 2013 samples. Alkalinity was measured on site by titration with bromophenol blue and 0.03N HCl.

Samples from 2015, 2016, and 2017 periods were analyzed at the U.S. Geological Survey (USGS, Boulder, Colorado, USA) laboratories by ICP-OES (PerkinElmer 7300 DV) for cations and IC (Dionex DX 600) for anions. Alkalinity was determined in the laboratory by automated titration (Thermo, 940-960 autotitrator) using standardized 0.01N H_2SO_4.

3.1.1.2. Fe and As redox speciation (collection, preservation and analysis)

The samples from 2011, 2012, and 2013 were only analyzed for Fe(T) and As(T) by ICP-MS as described in section 3.1.1.1, while samples for iron and arsenic redox species (Fe(T), Fe(II), As(T), As(III)) were sampled in the sampling campaign of 2015, 2016 and 2017. These samples were filtered with 0.2 µm HV (Millex) filtration units by using a syringe in some cases and with polyethersulfone (GVS) 0.2 and 0.45 µm membrane filters using a filter holder (Thermo Scientific) and manual pump. Preservation of arsenic species was made by adding 1% (v/v) 6 M HCl to the sample preserved in opaque polyethylene bottles (125-mL) which were previously soaked in 5% HCl and rinsed 3 times with deionized water. The samples were immediately stored in a cooler at 4º C after sampling and in refrigerator until analysis.

Iron and arsenic redox species were determined at the U.S. Geological Survey (Boulder, Colorado) laboratories. Total dissolved iron (Fe(T)) and ferrous iron (Fe(II)) concentrations were measured by the colorimetric FerroZine method (To et al., 1999) with a Hewlett Packard 8453 diode array UV/VIS spectrophotometer. Total dissolved arsenic (As(T)) and dissolved arsenite (As(III)) concentrations were determined with a Perkin Elmer (FIAS 100) hydride generation atomic absorption spectrometry system (HG-AAS) using the method described by McCleskey et al. (2003).

3.1.1.3. Geochemical modeling and statistical treatment of the data

226 Saturation indices for water samples were calculated with PHREEQC.v3 (Parkhurst and Appelo
227 2013). The statistical analysis of the data consisted in calculations of mean, maximum,
228 minimum, and range values. Ions rates (Na/K) were also calculated.

229 *3.1.2. Lacustrine sediments and secondary minerals samples*

230 One sediment sample (LS-1) of 1kg weight was taken in the south area of the Los Pozuelos
231 lagoon in the dry season of 2013 next to the lagoon water sampling site (PL-1-2013) (Fig. 1 D).
232 The sediments were preserved in a cooler at 4º C after sampling and immediately dried at room
233 temperature and fractioned for analysis. In the laboratory USGS (Boulder, Colorado) the
234 sediments were completely digested and total arsenic was analyzed by HG-AAS with a Perkin
235 Elmer (FIAS 100). Three different certified standard reference materials (SRM-Mess-1
236 (Canadian), SRM-2702-Marine sediments (NIST), and SRM-8704 Buffalo river sediment
237 (NIST)) were used. The detection limit for As was 0.25 mg/kg.

238 In the dry season of 2015 200g samples of fine fluvial sediments with abundant secondary iron
239 precipitates were taken from SM-1 and SM-2 sites in Peñas Blancas River flood plain (Fig 1 C).
240 The samples were preserved in a cooler at 4º C after sampling and immediately dried at room
241 temperature and fractioned for analysis. These samples were digested and analyzed for total As
242 with the same procedure described above for the lacustrine sediments. These samples were also
243 analyzed by quantitative XRD at USGS Boulder laboratories with a Siemens D500 X-ray
244 diffractometer from 5° to 65° 2θ using Cu Kα (λ = 1.54056 Å) X-ray radiation with a step size of
245 0.02 degrees and a dwell time of 2 seconds per step. Quantitative mineralogy was calculated
246 using the USGS software, RockJock (Eberl, 2003), which fits XRD intensities of individual
247 mineral standards to the measured diffraction pattern.

248 Moreover, samples of efflorescent salts were taken in Peñas Blancas River (SM-3) and in the
249 surface of soils in the vicinity of W8 well (SM-4) (Fig. 1 C). The samples were taken with plastic
250 spoons and preserved in sealed polyethylene tubes in a refrigerator under dark conditions to
251 prevent changes by oxidation and/or dehydration. These samples were analyzed by qualitative
252 XRD at USGS Boulder laboratories with a Siemens D500 X-ray diffractometer from 5° to 65° 2θ
253 using Cu Kα (λ = 1.54056 Å) X-ray radiation with a step size of 0.02 degrees and a dwell time of
254 2 seconds per step. The mineralogy was identified using Jade software (MDI, version 9) and the
255 International Centre for Diffraction Data (ICDD) 2003 database.

256 **4. Results and discussion**

257 *4.1. Hydrogeological and geochemical characterization of surface waters and groundwater in*
258 *Pozuelos basin*

259 *4.1.1. Rivers*

260 Cincel and Santa Catalina are the most important rivers in Pozuelos basin, their headwaters are in
261 the south and northwest areas of the basin, respectively, discharging their waters into Los
262 Pozuelos lagoon (Fig. 1). The Cincel River is the main source of surface water to the lagoon. The
263 discharge of the rivers was mainly measured in the dry season when the field conditions permit
264 access to most of the sites. In the headwaters of the Cincel River the discharge is permanent and
265 vary between 0.13 – 0.52 m^3/s, but in the mid areas of the basin there is infiltration with very low
266 to no discharge (Table 1). The runoff increases again in the vicinity of the lagoon with values
267 between 0.08 – 0.26 m^3/s. In the headwaters of Santa Catalina River, the discharge was measured
268 before and after the town of Santa Catalina with values of 0.10 and 0.21 m^3/s respectively. In the
269 mid areas of the basin there is also infiltration and its runoff increases again at the lagoon
270 discharge with extremely low flow velocity. During the wet season, runoff increases all along the

rivers. The discharge values for Santa Catalina and Cincel Rivers were measured previously between 1992-1996 by Paoli et al. (2011). Similar values were determined in the headwaters of Santa Catalina River for dry season (0.3 m^3/s) while a strong increment was measured for wet season (0.9 m^3/s). In Cincel River the discharge measurements were made in the proximity of Pan de Azúcar mine showing also low values for dry season (0.1 m^3/s) and higher values in wet season (0.5 m^3/s) (Paoli et al., 2011).

The pH values observed in rivers have a mean value of 8.16. In general, the tendency is that the pH increases from the headwater of the rivers to its discharge in the lagoon. This trend is likely caused by calcite dissolution with some enhancement from evaporation. The mean value for calcite saturation indices in rivers is -0.89. For sites CR-5, CR-6, and CR-7 in the Cincel River, close to the discharge to the lagoon, the mean of calcite saturation indices is 0.21. The conductivity increases from the headwaters of the rivers to the center of the basin. The headwaters of the Cincel and Santa Catalina Rivers show the lowest conductivity values of 139.7 and 227 µS/cm respectively, which increase in the discharge to the lagoon to a maximum of 352 and 448 µS/cm respectively (Table 1).

The Piper diagram for river waters can be seen in Figure 3. The water type of most of the rivers is mainly Na-HCO_3 with increments in Ca in some cases (Table 1). Sodium is the dominant cation, with concentrations from 13.7 to 47.6 mg/l (Table 1). This water type is common during weathering of crystalline bedrock in arid environments. In general, HCO_3 > SO_4 > Cl > F > NO_3 > PO_4 and Na > Ca > Mg > K. However, Santa Catalina River has a composition which is mainly Ca-Na-SO_4 as well as Guayatayoc River (GR-DS) (Table 1). Total iron concentration in rivers is low and varies between 5 – 210 µg/L, when measured, the concentration of ferrous iron (Fe(II)) is higher than ferric iron (Fe(III)), except for Santa Catalina River (SCatR-2-DS; SCatR-3-DS)

294 (Table 2). Guayatayoc and Peñas Blancas Rivers, show some of the highest iron concentrations
295 in the basin (94 µg/L and 90 – 210 µg/L respectively), probably related to oxidizing sulfide
296 sources. In Guayatayoc River sulfide (i.e. pyrite) mineralized shales were observed in the fluvial
297 sediments during the sampling campaigns.

298 *4.1.2. Groundwater*

299 The water table in the sampled wells varied between 1 - 7 m depth in the dry season, to 0.2 - 2.5
300 m depth in the wet season. The wells located in the upper to middle areas of the basin (W1, W2,
301 W3, W4, W5, W7, W11, W12, W13, W15, W16) are situated on Pleistocene - Holocene coarse
302 alluvial-alluvial fan deposits (Fig. 1). Wells located in the middle to lower area of the basin (W6,
303 W8, W9, W14) are situated on the lacustrine lagoon deposits.

304 The pH of groundwater is circumneutral to basic with a mean value of 7.55. The conductivity
305 ranges between 131 – 1355 µS/cm increasing from the upstream wells to the lower area of the
306 basin (Table 3). The composition of groundwater is mainly Ca-HCO_3 and Na-HCO_3 (Fig. 3). In
307 general, HCO_3 > SO_4 > Cl > F > NO_3 > PO_4 and Ca > Na > Mg > K. However, some wells show
308 a composition where SO_4 increases in some periods, like well W4. During the dry season of 2013
309 where the W4 composition is Ca-SO_4 suggesting dissolution of gypsum, the gypsum saturation
310 indix calculated is -1.59. For well W9, the composition changes from Na-HCO_3 to Na-SO_4
311 during the dry season of 2013 and 2015. The increase in SO_4, Na, and TDS from high to low
312 basin reflects the normal evolution of groundwater in closed basins (Eugster and Jones, 1979;
313 Deocampo and Jones, 2014). For well W8, the composition of the groundwater varies from Ca-
314 HCO_3 in wet season to K-HCO_3 in dry season with Na/K rates of 0.2 and 0.3, which is well
315 correlated with the precipitation of Na rich white salts in the surface of the soils in the vicinity of
316 the well W8. These salts are composed of (in decreasing order of abundance) thenardite

317 ($Na_2(SO_4)$) + halite (NaCl) + Eugsterite ($Na_4Ca(SO_4)3{\cdot}2(H_2O)$) + scarce calcite ($CaCO_3$) and
318 gypsum ($CaSO_4 \cdot H_2O$). Efflorescent salts in the flood plain of Peñas Blancas river close to well
319 W4 have a similar composition, in decreasing order of abundance these salts are compose of
320 thenardite + halite + eugsterite + bloedite ($Na_2Mg(SO_4)_2{\cdot}4H_2O$) + scarce gypsum. Total iron
321 concentration is in general low (2 – 110 µg/L) except for well W8 where the concentration
322 increases to 1290 µg/L (Table 4). When measured, Fe(II) is the dominant species, except for
323 wells W8, W15, and W16 where the concentration of Fe(III) is higher (Table 4).

324 *4.1.3. Los Pozuelos Lagoon*

325 The surface of the lagoon was different in the different sampling dates, with the highest
326 extension in 2013 and 2015 and the lowest in 2016 and 2017 after five years of precipitation
327 below the annual mean (Fig. 4 A; B). Analyzing satellite images of the surface area of the lagoon
328 and the precipitation during the sampling period, surface areas not only vary between dry-wet
329 season, but they strongly depend on the amount of precipitation during summer (Fig. 4 A; B). If
330 the precipitation amount in summer was normal or close to the annual mean, the surface area of
331 the lagoon will not decrease so much by evaporation. Whereas a complete dry out of the lagoon
332 occurred after two or more consecutive years of low precipitation. This phenomenon was also
333 described by Igarzabal (1978).

334 Satellite and field observations indicate that during the driest periods, the waterbody of the
335 lagoon depend on the discharge of the Cincel River, being the main source of water to the lagoon
336 (Fig. 4 A).

337 Previous studies indicate that the salinity of the lagoon varies during the year and is influenced
338 by the seasonal climate (Mirande and Traccana, 2009; Rodriguez, 2012). Measurements made by
339 Rodriguez (2012) during winter and summer of 2009 indicate alkaline pH (8 – 10.4), and a wide

range of conductivity (219 – 1281 µS/cm), the lowest values correspond to wet season and the highest values to dry season. McGlue et al. (2013) measured a high concentration of solutes in the lagoon during the dry season of 2007 with a relatively large surface area. They determined Na-Cl water types, oxygen saturated waters, and basic pH (mean of 8.7).

In this work, the highest conductivity values of 1589 and 5600 µS/cm were measured when the lagoon was completely full in the dry season of periods 2013 and 2015 respectively. At that moment, the dominant ions were Na-Cl and the pH varied between 7.03 – 8.71 (Fig. A 4). In the periods 2016 and 2017 when the area of the lagoon was reduced and restricted to the proximity of the Cincel River discharge, the conductivity decreased to 288 and 344 µS/cm respectively, with a water type Na-HCO_3. At that time, the pH increased to values between 7.98 – 9.74 (Fig. 4 A). This pH behavior during extreme evaporation years is referred to as the pH divide (Drever, 1997). This phenomenon means that if the water in the lagoon has a pH greater than 7 (OH^- > H^+) and starts evaporating, the pH will steadily increase because the OH^- concentration keeps increasing from evaporation. If the initial pH is < 7 (H^+ > OH^-), the pH will steadily decrease with evaporation. In Figure 4 C, a plot of Na, Mg, Cl, conductivity and As vs the lagoon surface area was made to evaluate the evaporation effect. It is observed that when the lagoon surface is small the composition of the lagoon is very similar to Cincel River and mainly influenced by the river discharge (see composition of Cincel River in CR-7; Table 1). However, when the surface area of the lagoon increases, as in the periods 2015 and 2013 the effect of evaporation is evident by increasing the concentration of Na, Cl, Mg, conductivity, as well as the pH values in May-2015.

With the present study, we observe that the variation in the physical-chemical parameters of the lagoon is not only related to the annual dry-wet seasonal variation, but also to a larger inter-

annual scale process related to drier or wetter years affecting the total surface area of the lagoon and its physical-chemical parameters. In this sense, Magii and Navone (2009) indicate that the inter annual fluctuation of the surface area of the lagoon could be related to the El Niño–Southern Oscillation (ENSO). ENSO is a naturally occurring phenomenon involving fluctuating ocean temperatures in the central and eastern equatorial Pacific, coupled with changes in the atmosphere. This phenomenon has a major influence on climate patterns in various parts of the world and comprises three phases: El Niño (warm), La Niña (cold) and neutral. (World Meteorological Organization, 2014). Magii and Navone (2009), associated the retraction of the lagoon water body in the years 2002-2003 to dry periods during the El Niño 2002-2003. In the present study, the strong retraction of the lagoon observed between 2015 and 2016 (Fig. 4) could be also be related to a strong El Niño phase during 2015-2016 (Climate Prediction Center of United States).

4.2. Total arsenic and arsenic speciation

4.2.1. Rivers

In rivers, the total arsenic concentrations vary in a range from 1.46 to 27 µg/L (Table 1, Fig 5 B). The concentration of As in rivers increased from the headwaters to the center of the basin. The lower values were found in the headwaters of the rivers such as in Santa Catalina River (1.46 – 1.81 µg/L) and Cincel River (3.5 – 7.33 µg/L). The highest values were observed in Peñas Blancas River after acid mine discharge (27 µg/L) and in Cincel River in the discharge to the lagoon (17.8 – 20.3 µg/L). Arsenate (As(V) >> As(III)) is the dominant species in all river water samples (Table 1). Oxidation promotes higher As(V) concentration in rivers and also sorption in fluvial sediments.

385 Some sites like the Candado River (CaR-1), the Cincel River (CR-1, CR-5, CR-7), were
386 sampled between 3 and 5 times. At each sampling site, the concentration of As varied with time,
387 but the values remained in a similar range (Fig. 6).

388 *4.2.2. Groundwater*

389 Total dissolved As in groundwater ranges between 3.82 and 113 µg/L (Fig. 5 A). Regarding As
390 speciation, As (V) (arsenate) is the dominant species in groundwater (Table 4). The shallow
391 unconfined aquifer conditions promote oxidation and higher As (V) concentrations.

392 According to the Argentinian Alimentary Code (CAA), total dissolved As concentration in wells
393 W6 and W8 are above the limit for human consumption, which is 50 µg/L. However, according
394 to the World Health Organization, which recommended drinking water value is lower (10 µg/L)
395 most of the wells of the basin are not suitable for drinking purposes. Only wells W3, W12, W13,
396 W15 and W16 have concentrations of arsenic lower than 10 µg/L (Fig. 5 A).

397 A relation between the sedimentary facies of the aquifer and the concentration of arsenic is
398 observed (Fig. 5 A). It is noteworthy that the wells located in the lacustrine sediments show
399 higher concentration of As with a mean value of 44.6 µg/L, than wells located in non-lacustrine
400 alluvial-and alluvial fan deposits with a mean value of 13.6 µg/L (Table 4, Fig. 5 A). This
401 relation could be caused by the amount of water evaporation and, for that, water isotope analyses
402 ($\delta^{18}O_{H2O}$, δD_{H2O}) are needed and planned for future research.

403 Some wells (W2, W5, W6, W8, W9, W14) were sampled between 2 and 5 times according to
404 field accessibility, being W9 the most accessible and sampled site. For each site, the variation of
405 total dissolved As with time are shown in Figure 6. At each sampling site, the concentration of
406 As varies, but the values remain in a similar range. A general tendency of increasing arsenic

407 from the headwaters to the center of the basin can be observed (especially from wells W2 to
408 W8). However, in wells W14 and W9, closer to the lagoon, the concentrations of As decrease.
409 For well W8 lying in the lacustrine aquifer, the As concentration in the dry season (2013 and
410 2015 periods) were the highest (90.2 and 133 µg/L respectively). During the dry season, the
411 composition of the groundwater was K-HCO3 with Na/K ratio of 0.2 and 0.3. The
412 concentrations of As and K were found to increase towards the center of the basin and As
413 follows a linear regression with K (R2 = 0.767). In closed basins, K concentrations generally
414 increase towards the center of the basin, it is conserved in solution and it is eventually enriched
415 over Na through the precipitation of Na-rich saline minerals (Eugster and Jones 1979; Deocampo
416 and Jones, 2014). The presence of Na-rich efflorescence salts near W8 well were described
417 above in section 4.1.2. The concentration of arsenic decreases in the wet season with respect to
418 the dry season (Fig. 6). During the wet season the composition of the groundwater changed to
419 Ca-HCO3 and the concentration of As decreased to 74.3 µg/L. This trend could indicate a
420 tendency of decreasing arsenic by the effect of dilution by rainwater since the aquifer is very
421 shallow, and increasing arsenic during the dry season by evaporation. However, this variation is
422 not clearly observed in wells W9 and W2 because the value remains similar in both seasons.

423 *4.2.3. Los Pozuelos Lagoon*

424 In the lagoon, the concentrations of total dissolved As vary between 43.7 – 200.3 µg/L with
425 As(V) the dominant species. The higher As concentration was observed during the dry season of
426 May-2015 where the concentration increases up to 149.4 and 200.3 µg/L with As (III) the
427 dominant species (Table 2; Fig. 4 C).

428 The concentrations of As in the lagoon are the highest of all surface waters of the basin (Fig. 5 B
429 and 6 A). In this sense, high evaporation and the closed system effect most probably favor high

As concentrations in the lagoon. However, the abrupt increase of total dissolved As and the relative increase of As (III) during the 2015 period suggests another process that could be related to the biological activity in the lagoon -arrival of large numbers of flamingos (Fig. 4 C). Previous studies indicate that Los Pozuelos Lagoon is an important site for Andean Flamingo (*Phoenicopterus andinus*) and Puneño Flamingo (*Phoenicopterus jamesi,*) during the austral winter when other lagoons in the Altiplano-Puna are frozen, or late in dry season when other lagoons are dry (Rodriguez, 2012). Data from the bird's census performed at the lagoon from 2006 to 2019, shows 2015 as a year of high abundance, especially for flamingos with more than 100,000 individuals by the end of the dry season (Sistema de Información de Biodiversidad, 2019). In this case, bird guano and organic matter reduction could favor reduction of As(V) to As(III) (Campbell and Nordstrom, 2014), especially in the sediment pore waters and therefore increase the concentration of As in the lagoon. The high iron concentration which is 45-90% reduced in the lagoon when the arsenic concentration was high, also supports the concept of reducing conditions from increased organic matter or diffusion of As(III) from sediment pore waters.

4.3. Comparison with arsenic content in water of other basins in the Altiplano-Puna region

According to Tapia et al. (2019, this issue) a compilation of data of different water types in the Altiplano-Puna plateau shows that the highest concentrations of As are found in acid mine waters (0.003 – 117 mg/L), followed by brines (0.008 – 88 mg/L), and saline water (0.0002 – 29 mg/L), whereas the lowest values are found in groundwater (0.0001 – 6 mg/L) and rivers and lakes exhibit variable concentrations of As (0.0001 – 32 mg/L). Accordingly, in Los Pozuelos basin, acid mine waters from historical mining activity show the highest As concentrations in the basin (0.7 – 44 mg/l; Murray et al., 2014). The next highest are the lagoon saline waters where the

453 concentration goes up to 200 µg/L when the salinity of the lagoon increase, and to 43.7 µg/L
454 when the salinity decrease during dry years and river water is the main source of water of the
455 lagoon. Groundwater shows concentrations of As between 3.82 – 113 µg/L where the lowest
456 values are in alluvial-alluvial fan aquifer (3.82 – 29.7 µg/L) and the highest concentration are in
457 the lacustrine aquifer that surround the lagoon (10 – 133 µg/L). Finally, rivers show variable
458 concentrations of As (1.46 – 27 µg/L) increasing from the headwaters to the central area of the
459 basin.

460 Only a few studies have undertaken As speciation in waters of the Altiplano-Puna region (Tapia
461 et al., 2019, this issue). In San Antonio de Los Cobres, with circumneutral pH water (7.38), a
462 majority of the As was in its oxidized form As (V) (tap and river water waters) and the average
463 As concentration was 290 µg/L (Hudson-Edwards and Archer, 2012). In the Bolivian Altiplano,
464 oxidizing conditions were present in surface water and shallow groundwater, allowing As (V)
465 species to be dominant over As (III) species (Ramos et al., 2012; Ormachea et al., 2015). In
466 Pozuelos basin, As speciation measurements indicate that arsenate As (V) is the dominant
467 species in all water types. Only during one sample period for the lagoon, As (III) was observed
468 as dominant for a high water elevation of the lagoon and probably associated with reducing
469 conditions promoted by high concentrations of organic matter.

470 *4.4. Sources of As in Los Pozuelos basin waters*

471 *4.4.1. Pan de Azúcar mine (Pb-Ag-Zn)*

472 Anthropogenic sources of As like mining, increase the availability and mobility of As by
473 oxidative weathering of mine excavations, waste rocks and tailings (Bowell et al., 2014). Pan de
474 Azúcar (Pb-Ag-Zn) is an inactive mine located in the south area of Pozuelos basin (Fig. 1 A, and
475 SFig. 7 A). It constitutes an epithermal polymetallic deposit within adularia-quartz-sericite

476 hydrothermal alteration hosted in a middle Miocene (12 ± 2 Ma) dacitic volcanic dome (Segal
477 and Caffe 1999). It was exploited since colonial times until 1990, when the operation ceased
478 without setting any closure plan. About 70,000 m^3 of sulfide-rich tailings and waste surrounding
479 the mine is undergoing sulfide oxidation and acid water generation (Murray et al., 2014).
480 Nowadays it constitutes an anthropogenic source of arsenic to the surface waters and a potential
481 source to groundwater in the basin as well.

482 Pyrite and marcasite are the most abundant sulfides in the mine tailings (9.5 wt.%). Furthermore,
483 arsenic sulfide phases such as arsenopyrite (FeAsS) and freibergite, $(Ag,Cu,Fe)_{12}$ $(SbAs)_4S_{13}$, are
484 also present (Murray et al., 2014). In the primary zone of the tailings the As concentration is 623
485 mg/kg. After 25 years of oxidation, the amount of As in the oxidation zone of tailings ranges
486 between 92 – 236 mg/kg and it is associated with jarosite ($(Na, K, Pb)Fe_3(SO_4)_2(OH)_6$) and
487 schwertmannite (Murray et al., 2014), indicating As leaching.

488 Acid mine drainage with a pH = 2.1 – 4.06 and high As and metal concentrations (e.g. 0.7 – 44
489 mg/l As; 3.2 – 99.7 mg/l Cd; 0.4 –1.7 mg/l Cr; 10 – 21.3 mg/l Cu; 1.3 – 47mg/l Fe; 0.1– 1.4 mg/l
490 Pb; 388 – 8,960 mg/l Zn) drains from the tailings and discharges mainly into Peñas Blancas
491 River in the wet season (SFig. 7 B). During the wet season of 2012, it was possible to measure
492 the AMD discharge in Peñas Blancas River with a pH = 4.06 and an As concentration of 3.2
493 µg/L. This low concentration of As in AMD discharge observed during wet season is related to a
494 pH increase and As sorption in secondary iron precipitates (Murray, 2015). Upstream of the
495 AMD discharge, the presence of As (22.8 µg/L) with a high pH = 8.71 indicates a different
496 geogenic source of As and the possibility of As to remain in solution due to the decreasing
497 absorption capacity at basic pH (Campbell and Nordstrom 2014). Moreover, downstream of
498 AMD discharge, and because the relative runoff of AMD was lower than the Peñas Blancas

499 River runoff, the pH of the river remains high (8.36) and the As concentration increases up to 27
500 µg/L, being the highest value of As measured in river waters of this study. The pH in the Peñas
501 Blancas River remains high after AMD discharge and favors the solubility of As and its
502 migration downstream in the basin.

503 The X-Ray diffraction analyses for sediments from the flood plains of the Peñas Blancas River at
504 6 km downstream of the mine (SM-1 and SM-2) indicate the presence of secondary iron minerals
505 like schwertmannite and jarosite. The presence of these minerals indicates low pH (2 - 3.5)
506 conditions related to the AMD discharge, probably at the beginning of the wet season. The
507 amount of As determined in these sediments vary between 82 and 108 mg/kg of As. Because
508 flood plains are potential aquifer recharge zones, they are potential sources of As to the
509 groundwater.

510 Arsenic desorption from the surface of Al-, Fe- and Mn-oxyhydroxides (coating lithic fragments)
511 at high pH and mobilization as complex oxyanions (As and trace elements) in Na-HCO_3 type
512 groundwaters is mentioned in the Chaco-Pampean plain by Nicolli et al., (2012). Moreover,
513 reductive solubilization of As under water-saturated conditions by dissolution of As-bearing
514 Fe(III)-oxyhydroxides is likely the main cause for high solubilization of As in mining impacted
515 floodplains (Simmler et al., 2017). High concentrations of arsenic are found in groundwater
516 downstream of the mine (W4 = 21.4 µg/L; W8 = 113 µg/L), so it would be important to
517 understand or identify potential processes of arsenic desorption from secondary iron minerals in
518 the flood plains to the groundwater. Moreover, the major ion composition of groundwater in well
519 W4 (SO_4-Ca) could indicate the influence of acid mine drainage by an increase of SO_4 in the
520 groundwater. Analyses of environmental isotopes such as $\delta^{34}S_{SO4}$, $\delta^{18}O_{SO4}$ will be useful to better
521 understand the transport and effect of As from the mine site to groundwater.

522 *4.4.2. As-rich gold deposits in Rinconada Hill's shales*

523 Ordovician marine shales with very low grade of metamorphism are the most abundant rocks in
524 the basin and contain many epithermal and alluvial Au deposits (Fig. 1A) (Rodríguez et al.,
525 2001; Rodríguez and Bierlein, 2002). The origin of these deposits is linked to the main stage of
526 deformation, which occurred in the upper Ordovician – lower Silurian (Rodríguez et al., 2001).
527 Epithermal Au is hosted in small size quartz veins, which also are rich in pyrite and arsenopyrite.
528 The Au mineralization is structurally controlled and occurs typically along large anticline hinges.
529 Geochemical data indicate that these mineral deposits are rich in Au-As (Sb) and also contain
530 subordinate quantities of basic metals (Pb, Zn, Cu, and Mo; Rodriguez et al., 2001). Arsenic is
531 the main element that shows a strong correlation with hydrothermal gold mineralization
532 (Nordstrom, 2012; Reich et al., 2005; Zhu et al., 2011; e.g. Minas Azules-mineralized area and
533 Pasquiri), so this element may constitute a guide in the exploration of gold in the Puna
534 (Rodriguez et al., 2001).

535 Sulfides are not stable under aerobic conditions and oxidize to hydrous iron oxides with the
536 release of large amounts of sulfate, acidity, and associated trace constituents, including As
537 (Bowell et al., 2014). The dominance of SO_4 over HCO_3 in the head of Santa Catalina River
538 (SCatR-1 and SCatR-2) is related to the oxidation of sulfide in outcrops and alluvial deposits
539 according to the following reaction (Dold, 2010; Nordstrom et al., 2015):

540 $$FeS_2\ (s) + 15/4O_2\ (l) + 7/2H_2O\ (l) \rightarrow Fe(OH)_3\ (s) + 2SO_4^{2-}\ (aq) + 4H^+\ (aq)$$

541 High concentrations of sulfate are also observed in Lopiara River and Gayatayoc River, where
542 pyrite is observed on its fluvial sediments (SFig. 7 C). The oxidation of arsenopyrite and arsenic
543 release can be expressed as follows (Mok and Wai, 1994):

544 $$FeAsS\ (s) + 7/2O_2\ (l) + 4H_2O\ (l) \rightarrow Fe(OH)_3\ (s) + SO_4^{2-}\ (aq) + H_2\,AsO_4^{-}\ (aq) + 3H^{+}\ (aq)$$

545 During the oxidation of pyrite and arsenopyrite iron oxides are formed and can accumulate As up
546 to concentrations of several weight per cent (Bowell et al., 2014). There is a tendency of As to be
547 removed from the solution by co-precipitation in fluvial sediments especially when As (V) is the
548 dominant species (Campbell and Nordstrom 2014). Many iron oxide deposits were observed in
549 the fluvial sediments or fluvial channels of Santa Catalina River and Lopiara River for example.
550 The dominance of As (V) in the rivers could favor As adsorption to iron oxide deposits reducing
551 the amount of dissolved As that reaches the lagoon.

552 *4.4.3. Corranzulí Volcanic Complex ignimbrites*

553 Another source for As is related to effusive volcanic rocks in the surrounding area of Pozuelos
554 Basin, such as the Coranzulí ignimbrite volcanic rocks located in the headwaters of Candado
555 River (SFig. 7 D). The concentration of As in Candado River is higher (7.9 – 17 µg/L) than in
556 Cincel River (CR-1) in the confluence point (3.5 – 7.33 µg/L), indicating the contribution of As
557 from the ignimbrites rocks. Data from the nearest area indicates arsenic concentrations in the
558 range of 2.2 - 126 mg/Kg in these ignimbrites (Gorustovich et al., 1989). de Sastre et al. (1992)
559 pointed out that in the Puna the Tertiary and Quaternary volcanic rocks are natural sources of
560 arsenic in surface waters. Tapia et al. (2019, this issue) indicates that fluvial sediments originated
561 from Neogene volcanic rocks (i.e. ignimbrites) exhibited the highest concentrations of As when
562 compared to surficial sediments from other geologic periods and/or rock types. In addition, most
563 sediments exhibited higher concentrations of As (107 mg/kg average) than the upper continental
564 crust (5.7 mg/kg; Hu and Gao, 2008). It is unknown how As is hosted in the volcanic matrix of
565 the ignimbrites.

566 According to Key et al. (2010), the highest $^{87}Sr/^{86}Sr$ ratios at a given SiO_2 content in the most
567 peraluminous ignimbrites fit with a shale-like component in the northeastern Puna Granada–
568 Orosmayo–Cusi Cusi, Vilama, Panizos and Coranzulí magmas. Hence, because the shales are
569 already enriched in As (Rodríguez et al., 2001; Rodríguez and Bierlein, 2002), the source of As
570 of the ignimbrites could be derived from the shales.

571 *4.4.4. Lacustrine deposits, and influence of semi-arid conditions*

572 Because it is a closed basin, the As released from natural and anthropogenic sources is
573 transported in solution, and precipitated in the fluvial sediments and transported downstream to
574 be finally accumulated in the basin depocenter. As a consequence, higher concentrations of As
575 are found in groundwaters located in the lacustrine aquifer as well as in the lagoon waters and
576 the lagoon sediments. The concentration of As in the actual lagoon sediments is 24 mg/kg, four
577 times higher than the upper continental crust (5.7 mg/kg; Hu and Gao, 2008). However, this
578 value is lower than those found in other lake sediments in the Altiplano of Bolivia. Sediments of
579 Lake Uru Uru and Cala Cala Lagoon show a value of 56 mg/kg of As (Tapia et al., 2012).
580 According to these authors, this high value might be related to the metallogenic belts located in
581 the Eastern Andes Range. In these sediments As was mainly associated with iron oxides and
582 residual fractions (Tapia and Audry, 2013). In these lakes, the sediments act as a source of As in
583 the dry and wet seasons, with increased mobility during the wet season (Tapia and Audry, 2013).
584 The analysis of As in Los Pozuelos lagoon sediments was made in bulk samples and the
585 mineralogy of the sediments was not identified, but high organic matter content was observed.
586 As mentioned in section 4.2.3., high evaporation could increase As concentrations in the lagoon,
587 but the relative increase of As (III) during the 2015 period suggests biological reduction
588 processes (Campbell and Nordstrom, 2014). McGlue et al. (2012; 2013) indicates high organic

589 matter content in the sediments of the lagoon, with increasing values from the Cincel River delta
590 to the center of the lagoon. Moreover, their mineralogical analyses in surface and core sediments
591 of the lagoon indicates the presence of Fe-oxides and ungraded, massive, black pyrite-rich mud.
592 Oxidation-reduction processes and the presence of organic matter in Los Pozuelos lagoon can
593 influence the cycle of As by changes in the geochemistry of the water-sediment interphase,
594 which can contribute to the variability in the concentration of As in the lagoon.

595 **5. Conclusion**

596 In Los Pozuelos basin the As concentrations increases from the upstream areas to the center of
597 the basin in both surface and groundwater with the highest values observed in Los Pozuelos
598 Lagoon. Total dissolved arsenic in rivers varies in a range from 1.46 – 27 µg/L. In the lagoon,
599 the concentration of arsenic is highly variable (43.7 – 200.3 µg/L). High evaporation and the
600 closed system effect most probably increases As concentrations in the lagoon. However, the
601 abrupt increase of total dissolved As in May-2015 (up to values of 149.4; 200.3 µg/L), together
602 with an increase in As(III) and Fe(II) species, suggests that a process related to migratory birds
603 invasion that could increase the organic matter in the lagoon favoring arsenic reduction
604 increasing its solubility and concentration. In groundwater, the main source of drinking water for
605 the inhabitants of the basin, the arsenic concentrations vary between 8.22 – 113 µg/L. The wells
606 located in the external ring aquifer where alluvial-alluvial fan sediments are the dominant facies
607 have lower As concentrations (13.6 µg/L). The wells located in the internal ring aquifer where
608 lacustrine sediments are the dominant facies show higher concentration of As (44.6µg/L).
609 According to the World Health Organization, 70% of the wells have arsenic concentrations
610 above the recommended guideline (10 µg/L). According to the Argentinian Alimentary Code,
611 only two wells are above the limit for human consumption (50 µg/L).

612 Arsenate is the dominant species in all surface and groundwater, except for the lagoon where
613 variations between As (V) and As (III) species were observed and associated with organic matter
614 and reductive conditions in Los Pozuelos Lagoon.

615 There are at least three potential sources for As in surface and groundwater i) oxidation of As
616 sulfides in Pan de Azúcar mine wastes, and acid mine drainage discharging into the basin; ii)
617 weathering and erosion of mineralized shales; iii) weathering of volcanic eruptive non-
618 mineralized rocks located in the headwater of some of the streams.

619 Because it is a closed basin, the arsenic released from the natural and anthropogenic sources is
620 transported in solution, and in fluvial sediments, and finally accumulated in the center of the
621 basin where the concentrations increase because streams and sediment coalesce, and because of
622 evaporation. High evaporation rates that characterize a prolonged dry season in the basin most
623 probably favor As concentration increase in groundwater and the lagoon. Moreover, a larger
624 inter-annual scale process related to drier or rainy years most probably affects the total surface
625 area of the lagoon, its physical-chemical parameters, and the biological activity causing
626 variations in As concentration in the lagoon. Environmental isotopes ($\delta^{34}S_{SO4}$, $\delta^{18}O_{SO4}$, $\delta^{18}O_{H2O}$,
627 δD_{H2O}) in combination with water geochemistry are needed to better understand multiple As
628 sources, its mobility, and its behavior under semi-arid conditions. The data and interpretations of
629 how different geological, climatological, geochemical, anthropological, and biological processes
630 influence the presence and mobility of As in waters, as presented in this study, are transferable to
631 other closed basins in Central Andes, Latin America, and beyond.

632 **Acknowledgments**

633 We thank local inhabitants for allowing sampling in local wells. We specially thank to the people
634 of National Park Administration *(Monumento Natural Laguna de Los Pozuelos)* for her

assistance with the field work, sampling campaigns, and accommodation during field trips. The Environmental and Mining Secretaries of Jujuy Province authorized permits to the develop this study. A Fulbright travel grant partially financed a D. K. Nordstrom field trip to the study area. This research was financed by the Argentinian projects CIUNSA 2262, 1674, PICT 2015-1069, PIP 201101-189 and PIP 201101-133 and the USGS National Research Program. We also thank Dr. Geraldo Boaventura from Instituto de Geociencias, Universidad Nacional de Brasilia for anion (2013 samples) determination. We thank Kate Campbell as well for the XRD analysis at the USGS laboratory in Boulder, CO.

Author Contributions

JM, DKN, BD, and AK performed the sampling campaigns, laboratory work, and contributed to the interpretation, discussion of data, figures confectioning, and redaction of the manuscript. MRO contributed to the treatment of long term data and discussion. Blaine McCleskey is gratefully acknowledged for assistance and use of the USGS laboratory in Boulder, CO.

Conflict of Interest

The authors declare no conflicts of interest.

References

Agricultural and Industry Ministry of Argentina, IDE visor, Rinconada Jujuy, http://ide.agroindustria.gob.ar/visor/. [last accessed 12 March 2019].

Alcalde, J., C., 2008. Acuífero transfronterizo Puna, área Jujeña, in: Coira, B., and Zappetini E. O. (Eds.), Geología y Recursos Naturales de la provincia de Jujuy. Relatorio del XII Congreso Geológico Argentino Jujuy 2008. Imprenta DEL SRL, Buenos Aires. pp. 551-555.

657 Allmendinger, R. W., Jordan, T., E., Kay, S., M., Isacks, B. L., 1997. The Evolution of the
658 Altiplano-Puna Plateau of the Central Andes. Annual Review of Earth and Planetary
659 Sciences 25, 139–174. http://doi.org/10.1146/annurev.earth.25.1.139
660 Bianchi, A., R., Yañez, C., E., 1992. Las Precipitaciones en el Noroeste Argentino, Rinconada
661 town.http://anterior.inta.gob.ar/prorenoa/info/resultados/Precip_NOA/base_precipitacione
662 s_noa.asp. [last accessed 12 March 2019].
663 Bowell, R., J., Alpers, Ch., N., Jamieson, H., E., Nordstrom, D., K., Majzlan, J., 2014. The
664 Environmental Geochemistry of Arsenic — An Overview —, in: Bowell, R. J., Alpers,
665 Ch, N., Jamieson H. E., Nordstrom, D. K., Majzlan, J. (Eds.), Reviews in Mineralogy and
666 Geochemistry, Arsenic: Environmental geochemistry, mineralogy, and microbiology 79,
667 pp. 1 – 16.
668 Bonaventura, S., M., Tecchi, R., Vignale, D., 1995. The vegetation of the Puna Belt at Laguna
669 de Pozuelos Biosphere Reserve in northwest Argentina Vegetatio 119, 23-31
670 https://doi.org/10.1007/BF00047368
671 Bundschuh, J., Litter, M., I., Parvez, F., Román-Ross, G., Nicolli, H., B., Jean, J.-S., Liu, C.-W.,
672 López, D., Armienta, M., A., Guilherme, L., R., G., Cuevas, A., G., Cornejo, L., Cumbal,
673 L., Toujaguez, R., 2012. One century of arsenic exposure in Latin America: A review of
674 history and occurrence from 14 countries. Science of the Total Environmen. Special
675 Section - Arsenic in Latin America, An Unrevealed Continent: Occurrence, Health
676 Effects and Mitigation 429, 2–35. https://doi.org/10.1016/j.scitotenv.2011.06.024
677 Caffe, P., Coira, B., Chayle, W., Diaz, A., Martinez, M., Orosco, O., Perez, A., Perez, B.,
678 Ramirez, A., Rosas, S., 2001. Hoja Geológica 2366-I, Mina Pirquitas. Provincia de Jujuy.

679 Instituto de Geología y Recursos Minerales, Servicio Geológico Minero Argentino.
680 Boletín. Buenos Aires. 269 p.
681 Cajal, J., L., 1998. Las áreas naturales protegidas en la región andina correspondientes a la Puna
682 y Cordillera Frontal, in: Cajal, J. L., García Fernández, J., Tecchi, R., (Eds.), Bases para
683 la conservación y manejo de la Puna y Cordillera Frontal de Argentina: el rol de las
684 reservas de biosfera. UNESCO Regional Office for Science and Technology for Latin
685 America and the Caribbean, Uruguay, 2, pp. 25 – 42.
686 Camacho, M., Kulemeyer, J., J., 2017. The Quaternary of the Laguna de los Pozuelos Basin,
687 Northern Puna, Argentina, in: Rabassa, J. (ed.), Advances in Geomorphology and
688 Quaternary Studies in Argentina, Springer Earth System Sciences, Proceedings of the
689 Sixth Argentine Geomorphology and Quaternary Studies Congress, Springer Cham, pp.
690 237-259 http://doi.org/10.1007/978-3-319-54371-0
691 Campbell, K., M., Nordstrom, D., K., 2014. Arsenic speciation and sorption in natural
692 environments, in: Bowell, R.J., Alpers, C.N., Jamieson, H.E., Nordstrom, D.K. Majzlan,
693 J. (Eds.), Arsenic: Environmental Geochemistry, Mineralogy, and Microbiology,
694 Reviews in Mineralogy and Geochemistry, Reviews in Mineralogy and Geochemistry 79,
695 pp. 185 – 216.
696 Caziani, S., M., Derlindati, E., J., Tálamo, A., Sureda, A., L., Trucco, C., E., Nicolossi, G., 2001.
697 Waterbird Richness in Altiplano Wetlands of Northwestern Argentina. Waterbirds: The
698 International Journal of Waterbird Biology 24, (1) 103–117.
699 https://doi.org/10.2307/1522249
700 Cendrero, A., Díaz de Terán, J., R., González, D., Mascitti, V., Rotondaro R., Tecchi, R., 1993.
701 Environmental Diagnosis for Planning and Management in the High Andean Region: The

Biosphere Reserve of Pozuelos, Argentina. Environmental Management 17, (5), pp. 683-703. https://doi.org/10.1007/BF02393729

Climate Prediction Center. United States National Weather Service. NOAA. https://origin.cpc.ncep.noaa.gov/products/analysis_monitoring/ensostuff/ONI_v5.php. [last acceded 26 June 2019].

Código Alimentario Argentino (CAA), 2012, Capitulo XII, Bebidas Hídricas, Agua y Agua Gasificadas. [last acceded 13 March 2019]

Coira, B., Zappettini E., O., 2008. Mapa Geológico de la provincia de Jujuy. Servicio Geológico Minero Argentino, Instituto de Geología y Recursos Minerales. Buenos Aires.

Concha, G., Nermell, B., Vahter, M., 1998. Metabolism of Inorganic Arsenic in Children with Chronic High Arsenic Exposure in Northern Argentina, Environmental Health Perspectives 106, (6), 355–359. https://doi.org/10.1289/ehp.98106355

Concha, G., Broberg, K., Grandér, M., Cardozo, A., Palm, B., Vahter, M., 2010. High-Level Exposure to Lithium, Boron, Cesium, and Arsenic via Drinking Water in the Andes of Northern Argentina. Environmental Science & Technology 44, 6875–6880. https://doi.org/10.1021/es1010384

de Sastre, M., Varillas, A., Kirschbaum, P., 1992. Arsenic content in water in the Northwest area of Argentina, in: International Seminar Proceedings: Arsenic in the Environment and Its Incidence on Health. Santiago, Chile, pp. 91–99.

Deocampo, D., M., Jones, B., F., 2014. Geochemistry of saline lakes, in: Drever, J.I. (ed.), Treatise on Geochemistry, 2nd edition, v. 7, Surface and Ground Water, Weathering and Soils, Elsevier-Pergamon, Oxford, pp. 437 – 469.

724 Dold, B., 2010: “Basic concepts in environmental geochemistry of sulfide mine-waste
725 management”. In: Sunil Kumar (Ed.) “Waste Management”, ISBN 978-953-7619-84-8.
726 INTECH open access publications, 173-198.
727 http://www.intechopen.com/books/show/title/waste-management.
728 Drever, J., I., 1997. The Geochemistry of Natural Waters: Surface and Groundwater
729 Environments, 3rd ed., Prentice-Hall, New York.
730 Eberl, D., D., 2003. User guide to RockJock – A program for determining quantitative
731 mineralogy from X-ray diffraction data, USGS open file report 2003-78.
732 Eugster, H., P., Jones, B., F., 1979. Behavior of major solutes during closed-basin brine
733 evolution. American Journal of Science 279, 609 – 631.
734 Farías, S., S., Bianco de Salas G., Servant, R., E., Bovi Mitre, G., Escalante, J., Ponce, R., I.,
735 2009. Survey of arsenic in drinking water and assessment of the intake of arsenic from
736 water in Argentine Puna, in: Bundschuh J, Armienta MA, Birkle P, Bhattacharya P,
737 Matschullat J, Mukherjee AB, (Eds), Natural arsenic in groundwater of Latin America.
738 CRC Press/Balkema Publisher; Leiden, p. 397–407.
739 Garreaud, R., Vuille, M., Clement, A., C., 2003. The climate of the Altiplano: observed current
740 conditions and mechanisms of past changes. Palaeogeography, Palaeoclimatology,
741 Palaeoecology 194, 5–22. https://doi.org/10.1016/S0031-0182(03)00269-4
742 Gorustovich, S., Vullien, A., Aniel, B., Bustos, R., 1989. Uranio en relación a ignimbritas
743 Cenozoicas de la comarca Coranzuli-Ramallo, Puna Argentina. Asociación Geológica
744 Argentina Revista 44, 175–185.
745 Hu, Z., Gao, S., 2008. Upper crustal abundances of trace elements: A revision and update.
746 Chemical Geology 253, 205–221. https://doi.org/10.1016/j.chemgeo.2008.05.010

747 Hudson-Edwards, K., A., Archer, J., 2012. Geochemistry of As-, F- and B-bearing waters in and
748 around San Antonio de los Cobres, Argentina, and implications for drinking and
749 irrigation water quality. Journal of Geochemical Exploration 112, 276–284.
750 https://doi.org/10.1016/j.gexplo.2011.09.007
751 Igarzábal, A., P., 1978. La Laguna de Pozuelos y su Ambiente Salino. Acta Geológica Lilloana,
752 15, 79–103.
753 Igarzábal, A., P., 1991. Evaporitas cuaternarias de la Puna Argentina, in: Pueyo J.J. (Ed.),
754 Génesis de formaciones evaporíticas: Modelos Andinos e Ibéricos., Universitat de
755 Barcelona Pub, Barcelona 2, pp. 333–373
756 INDEC, 2010. Argentinian National Census
757 https://www.indec.gob.ar/nivel4_default.asp?id_tema_1=2&id_tema_2=41&id_tema_3=
758 135 [last accessed 12 March 2019]
759 Kay, M., S., Coira, B., L., Caffe, P., J., Chen, C., 2010. Regional chemical diversity, crustal and
760 mantle sources and evolution of central Andean Puna plateau ignimbrites. Journal of
761 Volcanology and Geothermal Research 198 (1–2), 81–111.
762 https://doi.org/10.1016/j.jvolgeores.2010.08.013.
763 Kirschbaum, A., Murray, J., Arnosio, M., Tonda, R., Cacciabue, L., 2012. Pasivos ambientales
764 mineros en el noroeste de Argentina: Aspectos mineralógicos, geoquímicos y
765 consecuencias ambientales. Revista Mexicana de Ciencias Geológicas 29, (1), 248–264.
766 Magii, A., E., Navone, S., M., 2009. Consecuencias de El Niño 2002 sobre las lagunas de
767 Trenque Lauquén y Pozuelos, in: Fernández Reyes, L., Volpedo A.V. Pérez Carrera, A.,
768 (Eds), Estrategias Integradas de Mitigación y Adaptación a Cambios Globales, Red

769 CYTED 406RT0285 Efecto de los cambios globales sobre los humedales de
770 Iberoamérica. Buenos Aires, pp. 185 – 191.
771 McCleskey, R., B., Ball, J., W., Nordstrom, D., K., 2003. Metal interferences and their removal
772 prior to the determination of As(T) and As(III) in acid mine waters by hydride generation
773 atomic absorption spectrometry: U.S. Geological Survey Water-Resources Investigations
774 Report 03-4117, 14 p. http://pubs.usgs.gov/wri/wri03-4117/
775 McGlue, M., M., Ellis, G., S., Cohen, A., S., Swarzenski, P., W., 2012. Playa-lake sedimentation
776 and organic matter accumulation in an Andean piggyback basin: The recent record from
777 the Cuenca de Pozuelos, North-west Argentina. Sedimentology 59, 1237–1256.
778 https://doi.org/10.1111/j.1365-3091.2011.01304.x
779 McGlue, M., M., Cohen, A., S., Ellis, G., S., Kowler, A., L., 2013. Late Quaternary stratigraphy,
780 sedimentology and geochemistry of an under filled lake basin in the Puna plateau
781 (northwest Argentina). Basin Research 25, 1–21. https://doi.org/10.1111/bre.12025
782 Mirande, V., Tracanna, B., C., 2009. Estructura y controles abióticos del fitoplancton en
783 humedales de altura. Ecología Austral 19, 119–128.
784 Mok, W., M., Wai, C., M., 1994. Mobilization of arsenic in contaminated river waters. in:
785 Nriagu J.O. (Ed.), Arsenic in the environment. Part I Cycling and characterization. John
786 Wiley Interscience, New York, pp. 99-108.
787 Murray, J., Kirschbaum, A., Dold, B., Mendes Guimaraes, E., Pannunzio Miner, E., 2014.
788 Jarosite versus Soluble Iron-Sulfate Formation and Their Role in Acid Mine Drainage
789 Formation at the Pan de Azúcar Mine Tailings (Zn-Pb-Ag), NW Argentina. Minerals 4,
790 (2), 477–502. https://doi.org/10.3390/min4020477

791 Murray, J., 2015. Procesos de oxidación de sulfuros, drenaje ácido de minas y movilidad de
792 metales en los diques de colas de la Mina Pan de Azúcar (Zn-Pb-Ag) y sus consecuencias
793 ambientales en la Cuenca de Pozuelos, Puna de Jujuy. Universidad Nacional de Salta,
794 Facultad de Ciencias Naturales. PhD thesis, 190 p.
795 Murray, J., Nordstrom, D.K., Dold, B., Kirschbaum, A., 2016. Distinguishing potential sources
796 for As in groundwater in Pozuelos Basin, Puna region Argentina. Arsenic Research and
797 Global Sustainability. Taylor & Francis Group, pp. 94–96.
798 National Parks Administration of Argentina. https://www.parquesnacionales.gob.ar/areas-
799 protegidas/region-noroeste/mn-laguna-de-los-pozuelos/ [last accessed 6 March 2019].
800 Nicolli, H., B., Bundschuh, J., Blanco, C., Tujchneider, O., C., Panarello, H., O., Dapeña, C.,
801 Rusansky, J., E., 2012. Science of the Total Environment Arsenic and associated trace-
802 elements in groundwater from the Chaco-Pampean plain, Argentina: Results from 100
803 years of research. Science of the Total Environment 429, 36–56.
804 https://doi.org/10.1016/j.scitotenv.2012.04.048
805 Nordstrom, D., K., 2012. Arsenic in the geosphere meets the anthroposphere, in J. Ng, B. Noller,
806 R. Naidu, J. Bundschuh, P. Bhattacharya (eds.), Understanding the Geological and
807 Medical Interface of Arsenic, Taylor and Francis, London, pp. 15-19.
808 Nordstrom, D., K., Blowes, D., W., Ptacek, C., J., 2015. Hydrogeochemistry and microbiology
809 of mine drainage: An update. Applied Geochemistry 57, 3–16.
810 https://doi.org/10.1016/j.apgeochem.2015.02.008
811 Ormachea, M., Bhattacharya, P., Šráček, O., Ramos, R., Eduardo, O., Quintanilla Aguirre, J.,
812 Bundschuh, J., Maity, J., P., R., 2015. Arsenic and other trace elements in thermal springs

813 and in cold waters from drinking water wells on the Bolivian Altiplano. Journal of South
814 American Earth Science 60, 10–20. https://doi.org/10.1016/j.jsames.2015.02.006
815 Parkhurst, D., L., Appelo, C., A., J., 2013, Description of input and examples for PHREEQC
816 version 3--A computer program for speciation, batch- reaction, one-dimensional
817 transport, and inverse geochemical calculations: U.S. Geological Survey Techniques and
818 Methods, book 6, chap. A43, 497 p., available only at http://pubs.usgs.gov/tm/06/a43.
819 Paoli, H., Elena, H., Mosciaro, J., Ledesma, F., Noé, Y., 2011. Caracterización de las cuencas
820 hídricas de las provincias de Salta y Jujuy – Cuenca "Cerrada de la Puna", Sub-Cuenca
821 "Pozuelos". Ediciones INTA, Salta, 5 p.
822 Plaza Cazón, J., Benítez, L., Murray, J., Kirschbaum, A., Kirschbaum, P., Donati, E., 2013.
823 Environmental Impact on Soil, Water and Plants from the Abandoned Pan de Azúcar
824 Mine. Advanced Material Research 825, 88–91.
825 https://doi.org/10.4028/www.scientific.net/AMR.825.88
826 Ramos, O., E., R., Cáceres, L., F., Muñoz, M., R., O., Bhattacharya, P., Quino, I., Quintanilla, J.,
827 Sracek, O., Thunvik, R., Bundschuh, J., García, M., E., 2012. Sources and behavior of
828 arsenic and trace elements in groundwater and surface water in the Poopó Lake Basin,
829 Bolivian Altiplano. Environment Earth Science 66, 793–807.
830 https://doi.org/10.1007/s12665-011-1288-1
831 Ramsar Site Information Service. Laguna de Los Pozuelos, site 555.
832 https://rsis.ramsar.org/ris/555?language=en [last accessed 6 March 2019]
833 Reich, M., Kesler, S., E., Utsunomyia, S., Palenik, C., S., Chryssoulis, S., L., Ewing, R., C.,
834 2005. Solubility of gold in arsenian pyrite. Geochimica et Cosmochimica Acta 69, 2781-
835 2796. https://doi.org/10.1016/j.gca.2005.01.011

836 Rodríguez, A., C., 2012. Dinámica superficial del Monumento Natural Laguna de los Pozuelos –
837 monitoreo de avifauna acuática implicancias para su conservación. Universidad Nacional
838 de Salta, Facultad de Ciencias Naturales. Grade thesis. 70 p.
839 Rodriguez, G., A., De Azevedo, F., I., Jr., Coira, B., Brodie, C., 2001. Mineralizaciones auríferas
840 en sedimentitas ordovícicas de la sierra de Rinconada (Jujuy-Argentina): implicancias
841 para la exploración minera. Revista geológica de Chile, 28, 47–66.
842 http://dx.doi.org/10.4067/S0716-02082001000100003
843 Rodríguez, G., A. , Bierlein, F., P., 2002. The Minas Azules Deposit—An Example of Orogenic
844 Lode Gold Mineralization in the Sierra de Rinconada, Northern Argentina, International
845 Geology Review 44:11, 1053-1067 https://doi.org/10.2747/0020-6814.44.11.1053
846 Rubiolo, D., G., 1997. Esquema de evolución tectonosedimentaria para las Cuencas Cenozoicas
847 de la Cordillera Oriental (22° a 23° lat. S.), Argentina. Acta Geológica Hispana 32, 77–
848 92.
849 Rubiolo, D., G, Seggiaro, R., Gallardo, E., Disalvo, A., Sánchez, M., Turel, A., Ramallo, E.,
850 Sandruss, A., Godeas, M., 1997. Hoja Geológica 2366-II / 2166-IV, La Quiaca.
851 Provincias de Jujuy y Salta. Instituto de Geología y Recursos Minerales, Servicio
852 Geológico Minero Argentino. Buenos Aires, Boletín 246, 113 p.
853 Schlebusch, K., Gattepaille, L., Engström, K., Vahter, M., Jakobsson, M., Broberg, K., 2015.
854 Human adaptation to arsenic-rich environments. Molecular Biology and Evolution 32 (6),
855 1544–1555. https://doi.org/10.1093/molbev/msv046.
856 Segal, S.J., Caffe, P., J., 1999. El grupo minero Pan de Azúcar, Jujuy, in Zappettini, E.O., (Ed.),
857 Recursos Minerales de la República Argentina, Instituto de Geología y Recursos
858 Minerales, Servicio Geológico Minero Argentino, Buenos Aires, 35, pp. 1579–1592.

Segal, S., J., Zappettini, E., J., Craig, 1997. Metalogénesis del oro de la Sierra de Rinconada, Provincia de Jujuy. Servicio Geológico Minero Argentino. Serie Contribuciones Técnicas, Recursos Minerales, Buenos Aires, 2, pp. 5-31.

Simmler, M., Bommer, J., Frischknecht, S., Christl, I., Kotsev, T., Kretzschmar R., 2017. Reductive solubilization of arsenic in a mining-impacted river floodplain: Influence of soil properties and temperature. Environmental Pollution 231, 722 – 731. https://doi.org/10.1016/j.envpol.2017.08.054

Sistema de Información de Biodiversidad, Administración de Parques Nacionales. 2019. Visor Web del Monitoreo de Aves Acuáticas en el área protegida Laguna de los Pozuelos. May 2019. [last acceded 2 July 2019]

Tapia, J., Audry, S., 2013. Control of early diagenesis processes on trace metal (Cu, Zn, Cd, Pb and U) and metalloid (As, Sb) behaviors in mining- and smelting-impacted lacustrine environments of the Bolivian Altiplano. Applied Geochemistry 31, 60–78. https://doi.org/10.1016/j.apgeochem.2012.12.006

Tapia, J., Audry, S., Townley, B., Duprey, J.L., 2012. Geochemical background, baseline and origin of contaminants from sediments in the mining-impacted Altiplano and Eastern Cordillera of Oruro, Bolivia. Geochemistry: Exploration, Environment, Analysis 12, 3–20. https://doi.org/10.1144/1467-7873/10-RA-049

Tapia, J., Murray, J., Ormachea, M., Tirado, N., Nordstrom, D., K., 2019. Origin, distribution, and geochemistry of arsenic in the Altiplano-Puna plateau of Argentina, Bolivia, Chile, and Perú. Science of the Total Environment 678, 309 – 325. https://doi.org/10.1016/j.scitotenv.2019.04.084

881 To, T., B., Nordstrom, D., K., Cunningham, K., M., Ball, J., W., McCleskey, R., B., 1999. New
882 method for the direct determination of dissolved Fe(III) concentration in acid mine
883 waters. Environment Science & Technology 33, 807-813.
884 http://doi.org/10.1021/es980684z
885 UNESCO Biosphere Reserves http://www.unesco.org/new/en/natural-
886 sciences/environment/ecological-sciences/biosphere-reserves/latin-america-and-the-
887 caribbean/argentina/laguna-de-pozuelos/ [last accessed 12 March 2019].
888 Western Hemisphere Shorebird Reserve Network. https://www.whsrn.org/laguna-de-los-
889 pozuelos [last accessed 12 March 2019].
890 World Meteorological Organization, 2014. El Niño/Southern Oscillation. Report 1145.
891 Chairperson, Publications Board. 12 p.
892 World View, earth data, NASA, United States.
893 https://worldview.earthdata.nasa.gov/?p=geographic&l=MODIS_Terra_CorrectedReflect
894 ance_Bands721,VIIRS_SNPP_CorrectedReflectance_TrueColor(hidden),MODIS_Aqua_
895 CorrectedReflectance_TrueColor(hidden),Reference_Labels(hidden),Reference_Features
896 (hidden),Coastlines&t=2018-06-26-T00%3A00%3A00Z&z=3&v=-
897 66.42288844174853,-22.536344499386328,-65.67252223081103,-22.172697038448828
898 [last acceded 15 March 2019]
899 Zhu, Y., An, F., Tan, J., 2011. Geochemistry of hydrothermal gold deposits: A review.
900 Geoscience Frontiers 2, 367-374. https://doi.org/10.1016/j.gsf.2011.05.006

901 Figures captions

902 Figure 1. (A)- Geological map of Los Pozuelos basin and sampling points of surface waters and
903 groundwaters. (B) - Zoom of sampling area in the upstream area of Cincel River. (C)-

Zoom of sampling are in the South-central area of the basin. (D)- Zoom of sampling are in the lagoon area.

Figure 2. Water balance of Los Pozuelos basin. P = precipitation; P-Evp = Potential Evapotranspiration; R-Evp = Real Evapotranspiration.

Figure 3. Piper diagram for surface waters and groundwater in Los Pozuelos basin.

Figure 4. A)- Variation in water surface, physical-chemical parameters, and total dissolved arsenic in Los Pozuelos Lagoon. Images from the Worldview NASA web site. B)- Precipitation histogram of Rinconada town showing the mean value of precipitation and the sampling dates of the lagoon precipitation data obtained from satellite information provided by the IDE Visor (Agricultural and Industry Ministry, Argentina). C)- Variation of Na, Cl, Mg, conductivity and As in the lagoon while increasing its surface area.

Figure 5. Arsenic concentrations in waters of Los Pozuelos basin. (A)- Groundwater. (B)- Surface waters. The lagoon represented points correspond to the lowest (PL-2 (2016)) and highest (PL-2 (2015)) concentrations of As measured in the lagoon.

Figure 6. Concentration of total dissolved arsenic in sites sampled multiple times, bars represent individual samples in different sampling periods. (A)- Surface waters. (B)- Groundwater.

Supplementary Figure 7. Representative pictures of anthropogenic and geogenic sources of arsenic in Los Pozuelos basin. (A)- AMD in Pan de Azúcar mine. (B)- AMD discharge in Peñas Blancas River (end of the wet season). (C)- Pyrite dissolution box wholes in rock fragments of Rinconada hill's shales (Lopiara River). (D)- Ignimbrite outcrops in the headwater of Candado and Cincel Rivers.

(A)

66 °

22 °

N

SCatR-2

SCatR-1

Santa Catalina River

W-16

Guayatayoc R.

GR

SCatR-3

W-15

Los Pozuelos lagoon

Rinconada Hill

Rinconada

Colquimayo River

CoIR

Cincel River

(D)

Cochinoca-Escaya Hill

Peñas Blancas R.

Pan de Azucar mine

(C)

(B)

Chajarahuaico River

Candado River

Km

0 15

Jujuy

Study area

Salta

Argentina

Legend

- River
- Acid mine drainage
- Los Pozuelos lagoon
- Riverbed and floodplain deposits (Holocene)
- Lacustrine deposits (Pleistocene-Holocene)
- Alluvial and alluvial fan deposits (Pleistocene-Holocene)
- Dacitic volcanic domes (Miocene)
- Limestone (Miocene)
- Tiomayo-Ignimbrites (Miocene)
- Coranzuli-Ignimbrites (Miocene)
- Sandstone and conglomerates (Oligocene)
- Sandstone and conglomerates (Cretaceous)
- Sedimentary-volcanic complex (Ordovician)
- Marine-shales (Ordovician)
- Au-epithermal
- Zn-Pb-Ag-Epithermal
- Au-Placer
- Pozuelos basin border
- River sampling points *(CR-1)*
- Groundwater sampling points *(W-1)*
- \# Lacustrine sediments *(LS-1)*
- * Iron secondary minerals and efflorescent salts *(SM-1)*
- Sampling areas (zoomed in on this map)

CoStr

LopR

Lopiara River

ChR

Chajarahuaico River

W-1

Cincel River

CR-1

CR-2

CaR-1

Candado River

2.5 km

(B)

W-13

W-14

W-9

CR-5

Colquimayo River

*SM-4

W-12

W-11

CR-4

W-8

W-6

CR-3

W-7

W-5

W-4

*SM-3

*SM-2

*SM-1

Peñas Blancas R.

Cincel River

PBR-1

PBR-2

W-3

W-2

3 km

(C)

PL-1-2016

PL-3-2015

PL-2-2015

CR-7

PL-1-2013

PL-1-2017

LS-1

PL-2-2016

Cincel River

CR-6

2.5 km

(D)

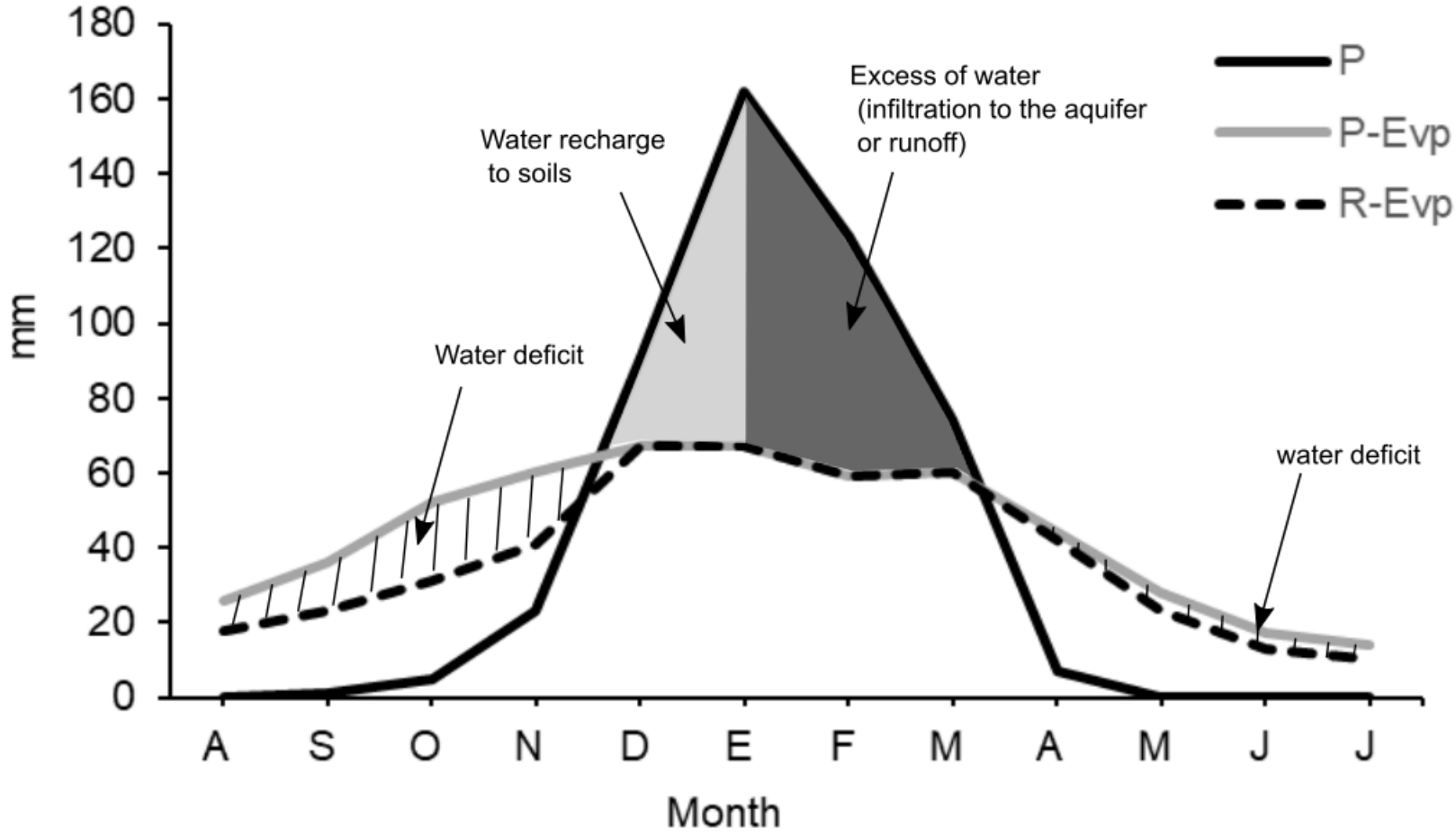
180
160
140
120
100
80
60
40
20
0
mm
A
S
O
N
D
E
F
M
A
M
J
J
Month
P
P-Evp
R-Evp
Water recharge
to soils
Excess of water
(infiltration to the aquifer
or runoff)
Water deficit
water deficit

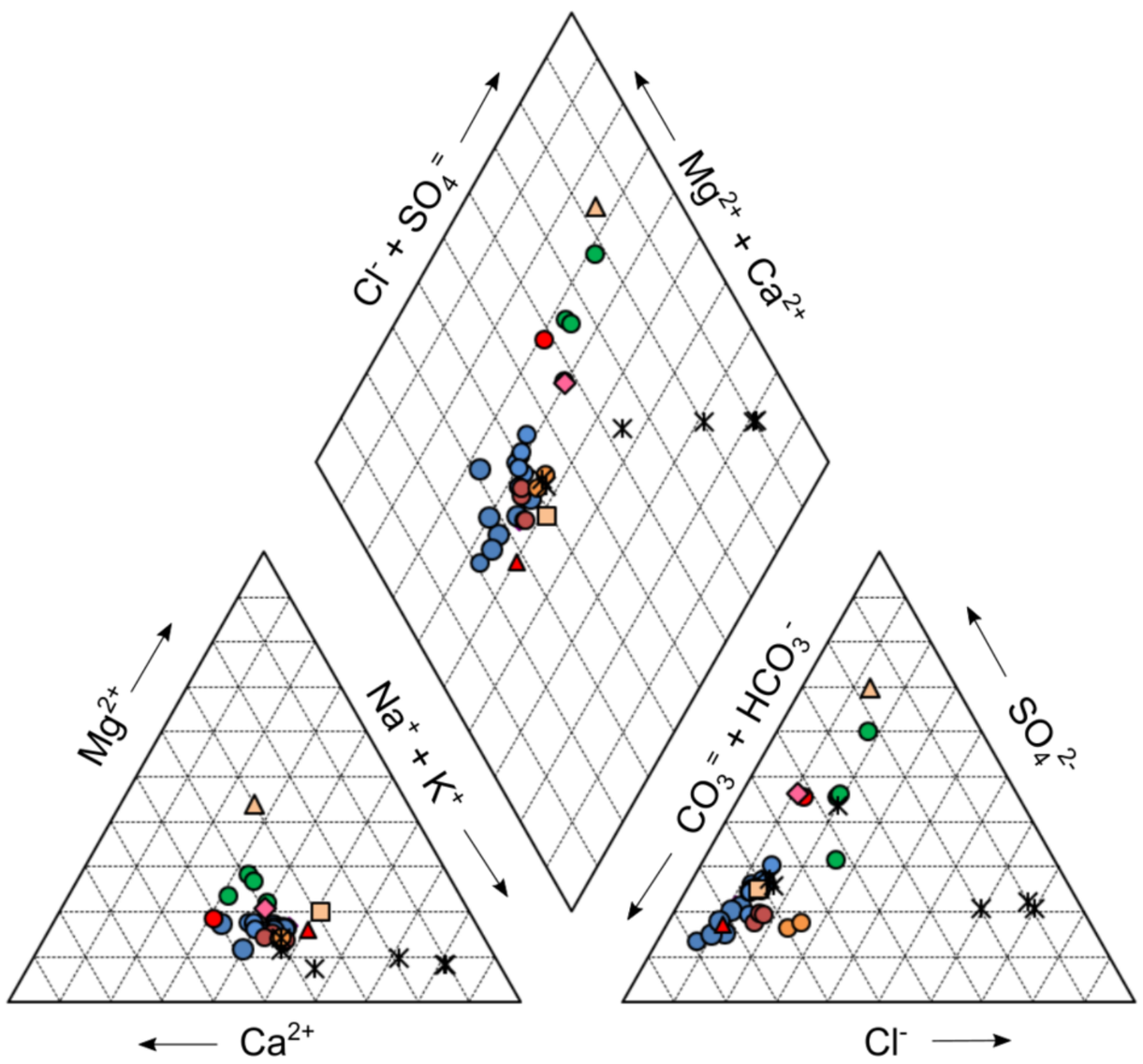

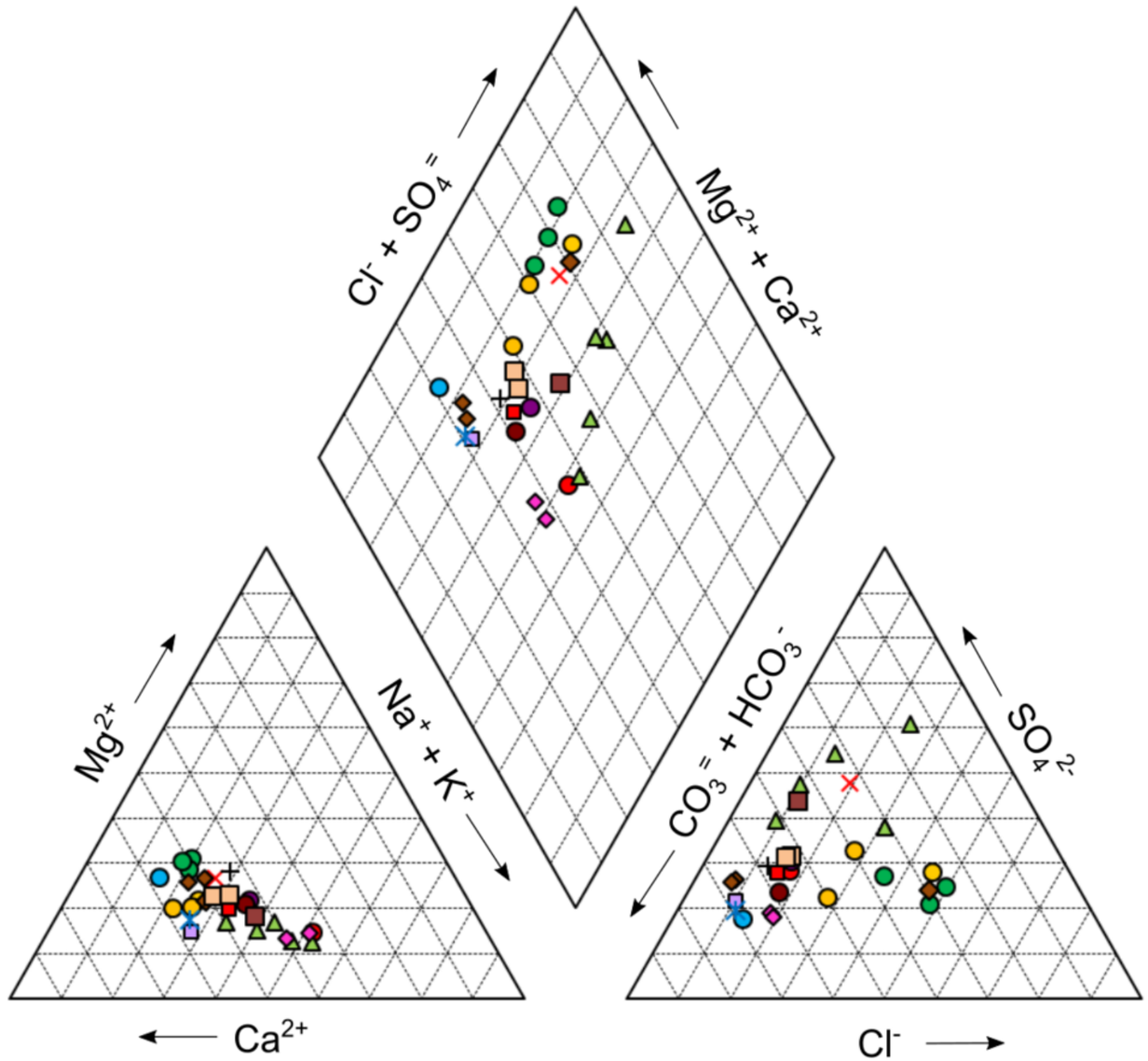

Surface water samples

- *Cincel River*
- *Candado River*
- *Santa Catalina River*
- *Colmayito Stream*
- *Chajarahuaico River*
- *Lopiara River*
- *Coquilmayo River*
- *Guayatayoc River*
- *Penas Blancas River*
- *Los Pozuelos Lagoon*

Groundwater samples

- *W1*
- *W2*
- *W3*
- *W4*
- *W5*
- *W6*
- *W7*
- *W8*
- *W9*
- *W11*
- *W12*
- *W13*
- *W14*
- *W15*
- *W16*

(A)

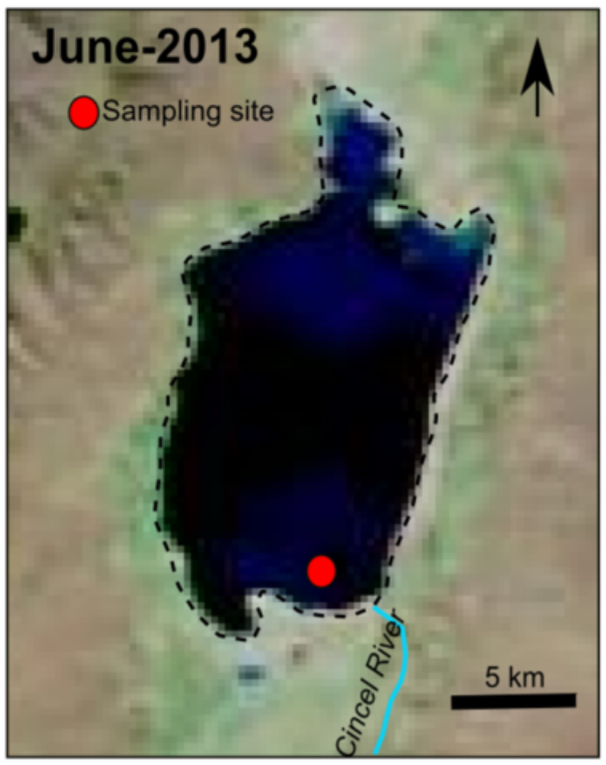

Water-type = Cl-Na
Conductivity = 1589 µS/cm
pH = 7.03
As = 47.5 µg/L

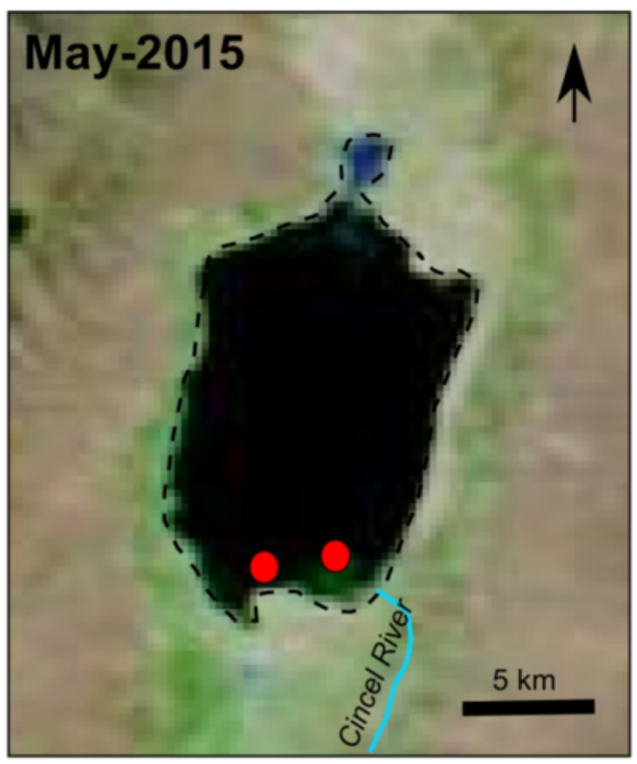

Water-type = Cl-Na
Conductivity = 5460; 5660µS/cm
pH = 8.68; 8.71
As = 149.4; 200.3µg/L

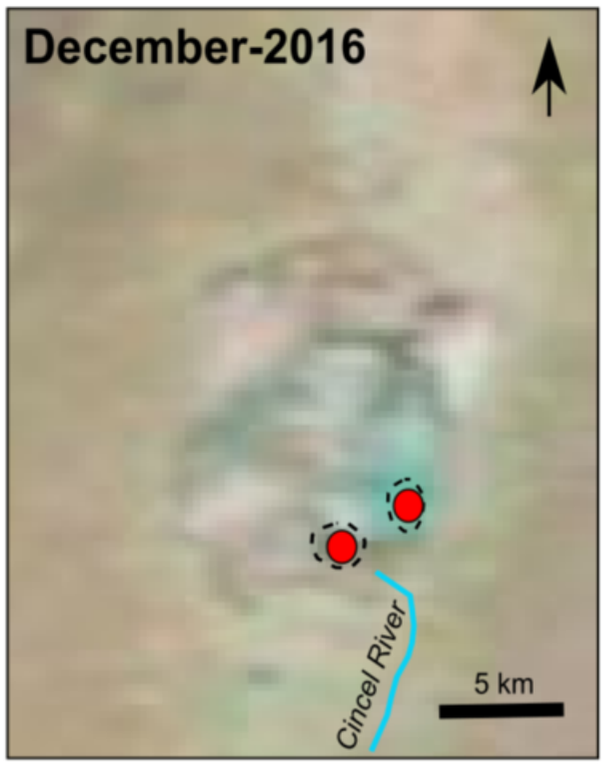

Water-type = HCO3-Na
Conductivity = 288; 365 µS/cm
pH = 7.98; 9.69
As = 43.7; 45.2 µg/L

Water-type = HCO3-Na
Conductivity = 344 µS/cm
pH = 9.74
As = 56.5 µg/L

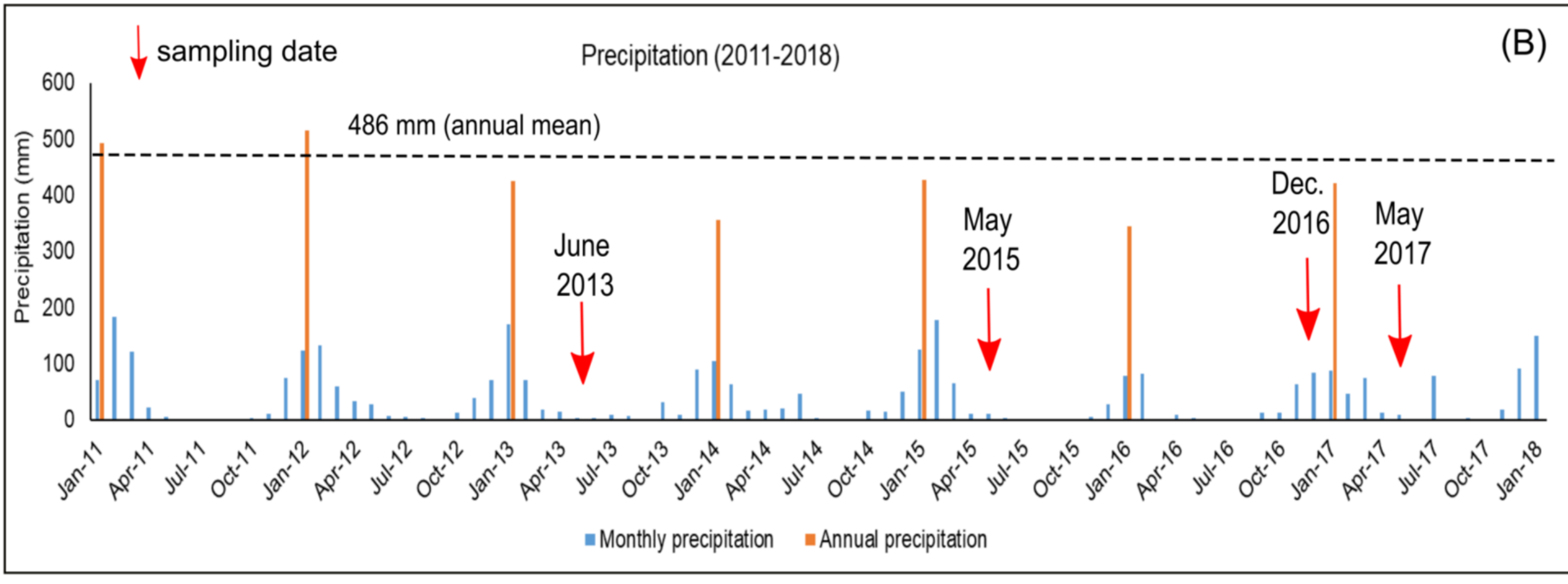

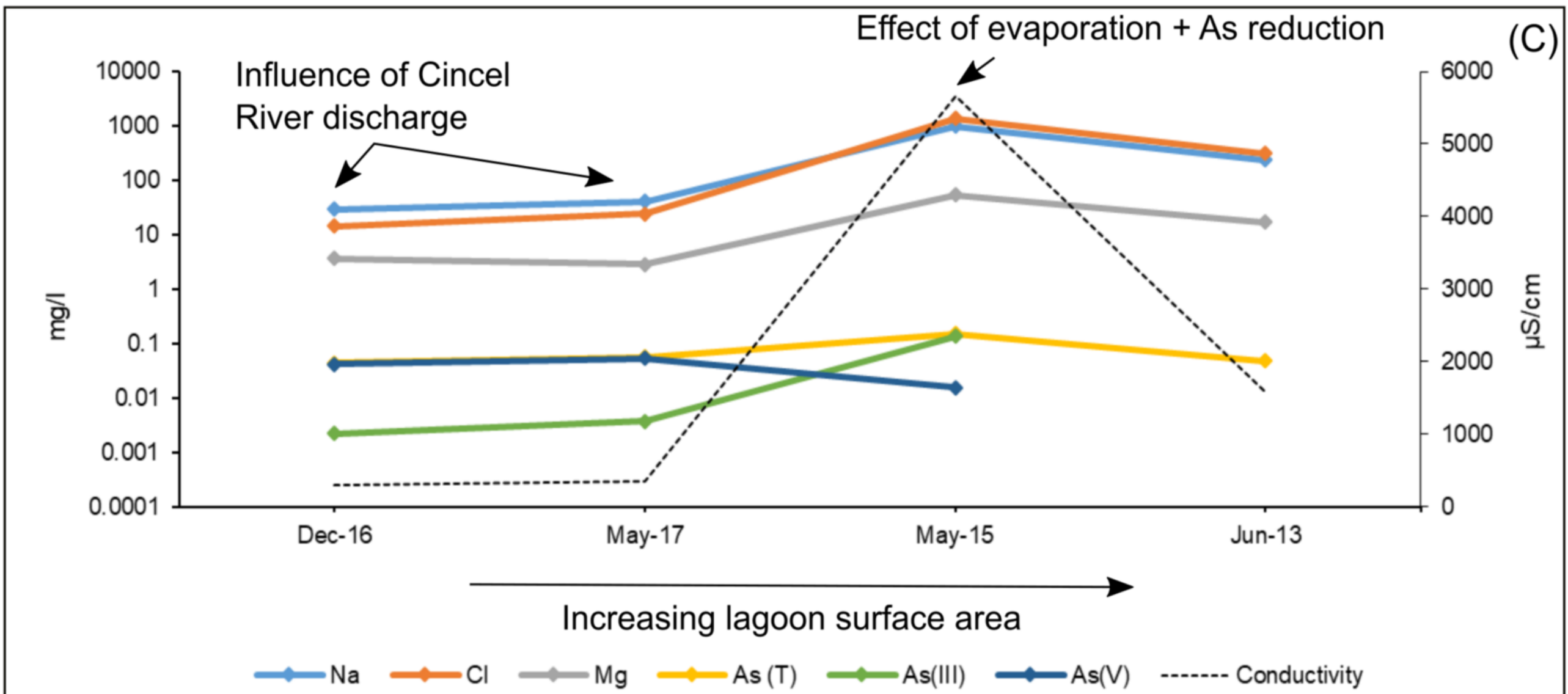

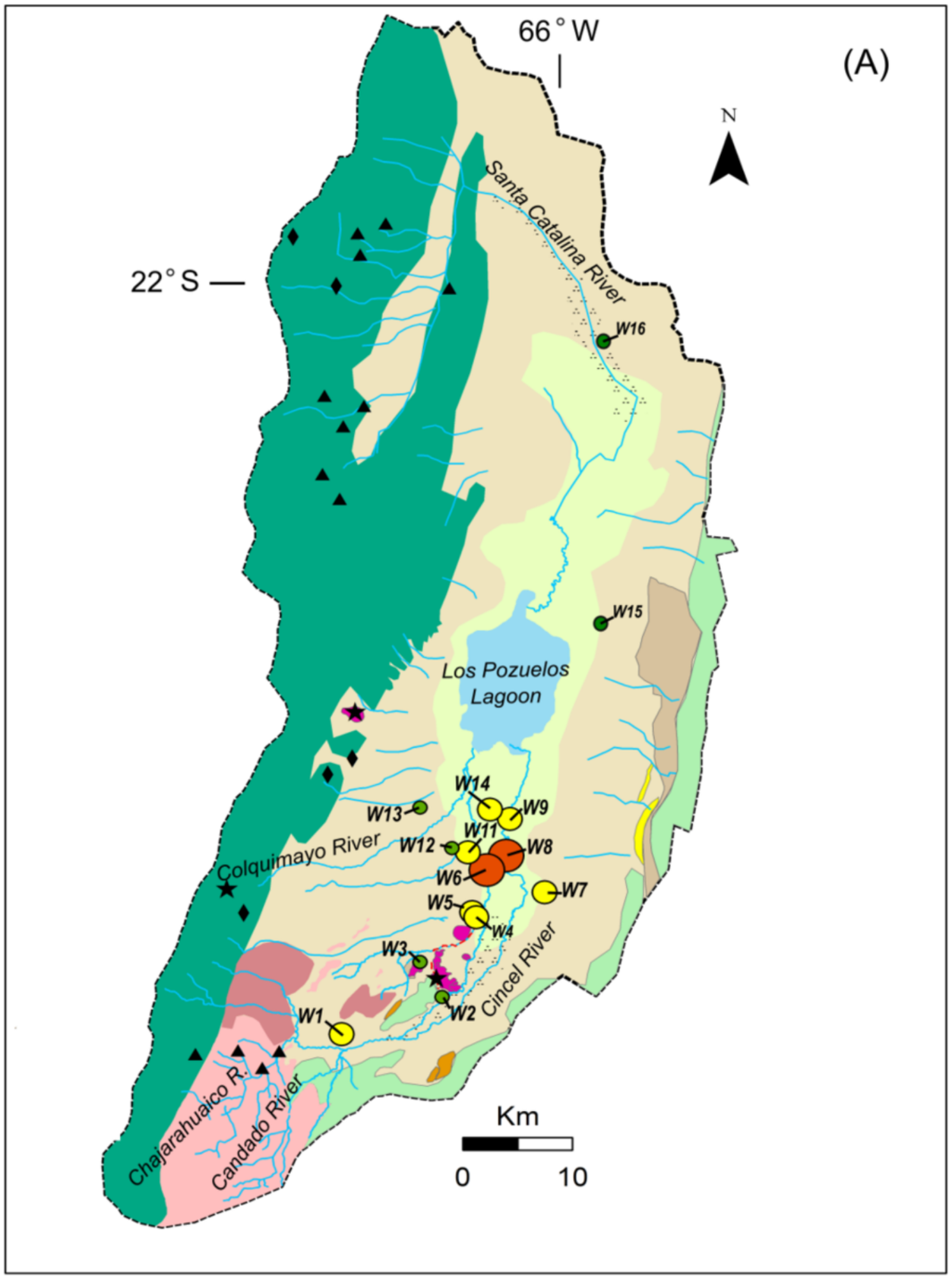

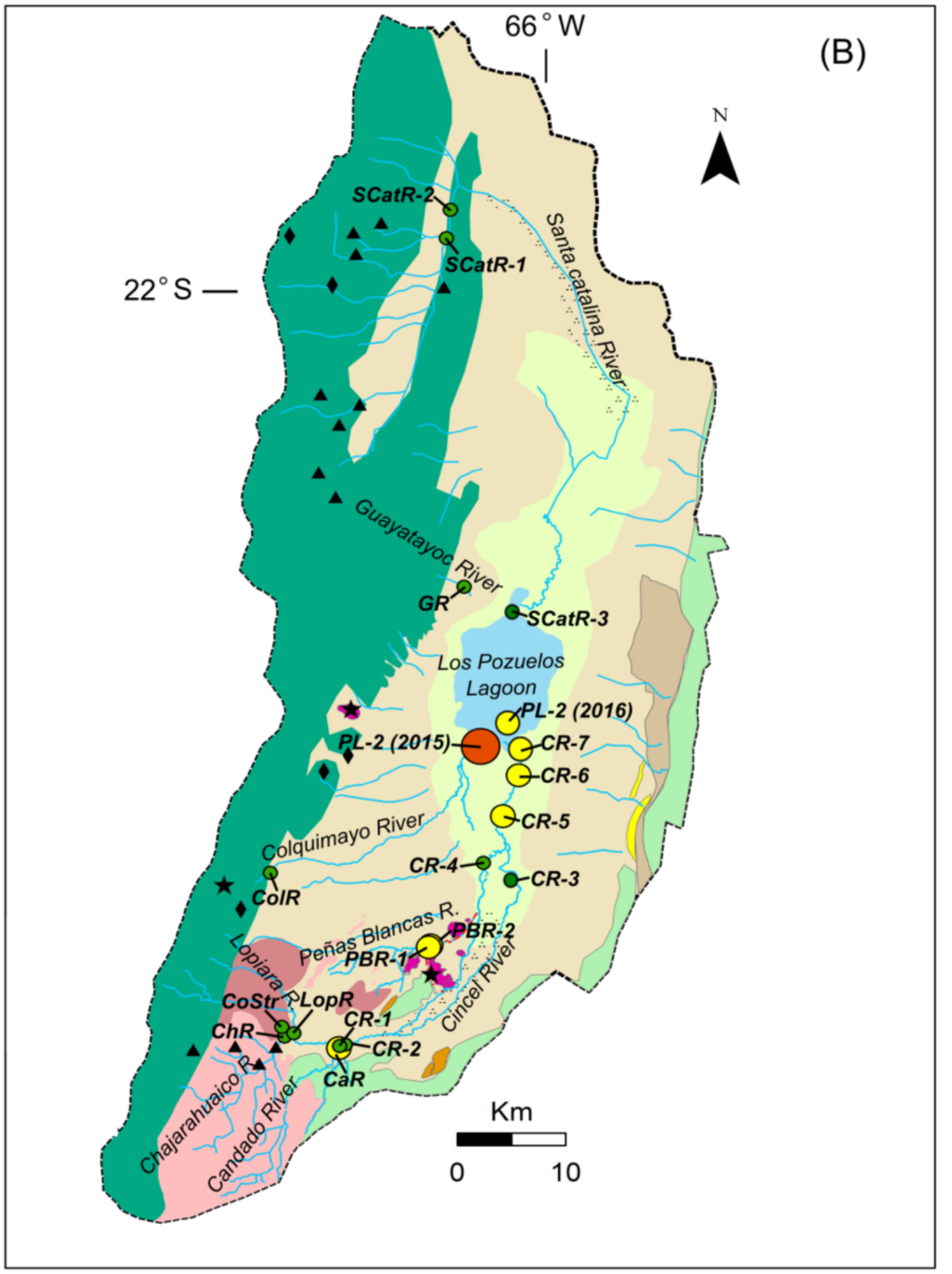

Legend

- River
- Acid mine drainage
- Los Pozuelos lagoon
- Riverbed and floodplain deposits (Holocene)
- Lacustrine deposits (Pleistocene-Holocene)
- Alluvial and alluvial fan deposits (Pleistocene-Holocene)
- Dacitic volcanic domes (Miocene)
- Limestone (Miocene)
- Tiomayo-Ignimbrite (Miocene)
- Coranzuli-Ignimbrites (Miocene)
- Sandstone and conglomerate (Oligocene)
- Sandstone and conglomerates (Cretaceous)
- Sedimentary-volcanic complex (Ordovician)
- Marine-shales (Ordovician)
- Au-epitermal
- Zn-Pb-Ag-Epithermal
- Au-Placer
- Pozuelos basin border

Arsenic concentration in waters

- < 10 µg/L
- 10 - 50 µg/L
- > 50 µg/L

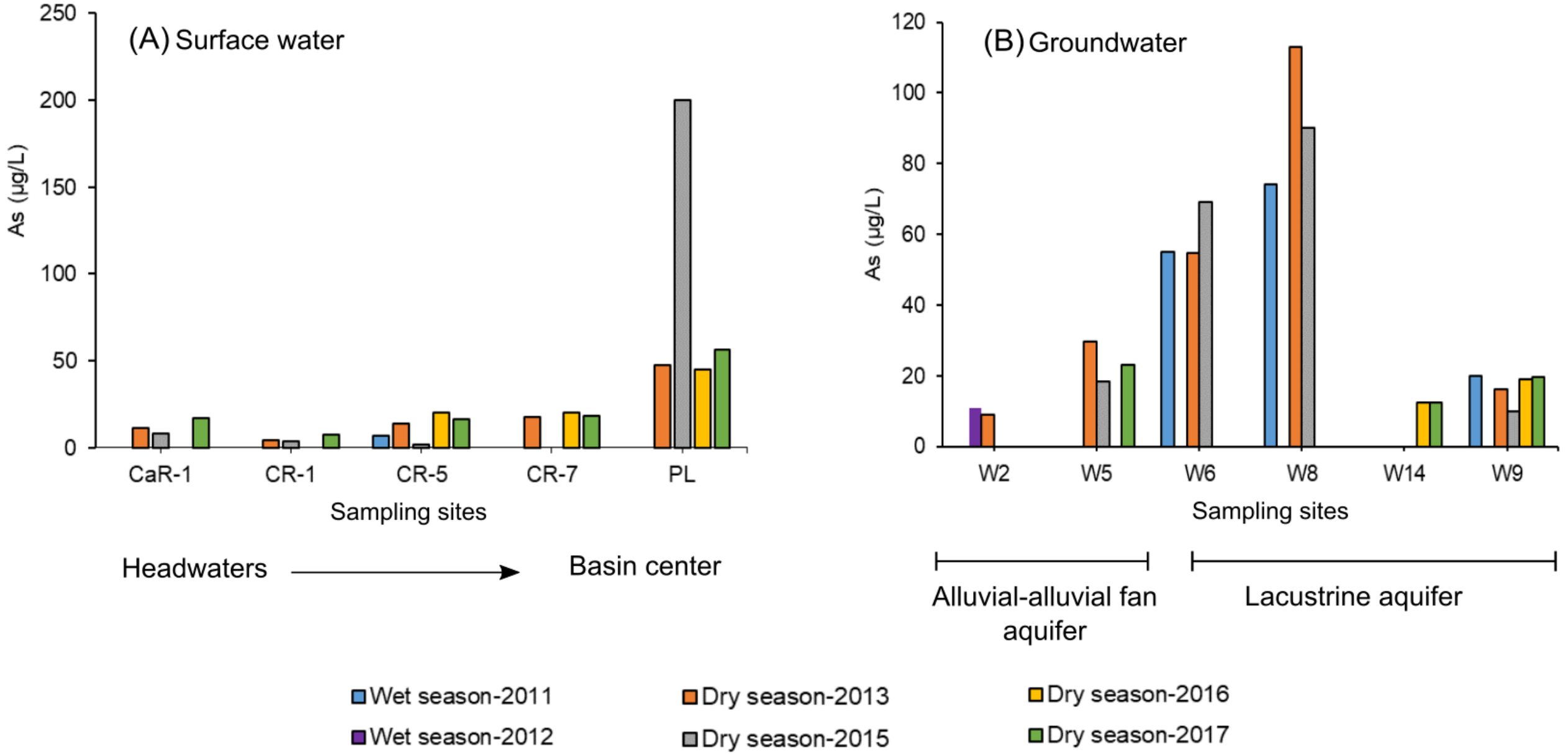
(A) Surface water
As (µg/L)
250
200
150
100
50
0
CaR-1
CR-1
CR-5
CR-7
PL
Sampling sites
Headwaters
Basin center
(B) Groundwater
As (µg/L)
120
100
80
60
40
20
0
W2
W5
W6
W8
W14
W9
Sampling sites
Alluvial-alluvial fan aquifer
Lacustrine aquifer
Wet season-2011
Wet season-2012
Dry season-2013
Dry season-2015
Dry season-2016
Dry season-2017

Table 1. Surface water samples, field parameters data and major ions analyses.

SAMPLE	Sampling date	Lat	Long	pH	T	Conductivity	TDS	DO	Discharge	Na	K	Ca	Mg	SO4	Cl	HCO3	NO3	PO4	F	Water-Type
					°C	µS/cm	ppm	mg/L	m^3/seg	mg/L	mg/L	mg/L	mg/L	mg/L	mg/L	mg/L	mg/L	mg/L	mg/L	
Cincel River																				
CR-1-DS	6/13/2013	22 40 58.5	66 08 11	6.99	5.8	152.8	n.d	2.3	0.52	13.7	1.81	10.9	2.9	10.92	4.34	80.52	<0.08	<0.2	<0.08	HCO_3-Na
CR-1-DS	5/1/2015	22 40 58.5	66 08 11	9.15	17.7	139.7	53.5	n.d	0.20	14.4	2.61	9.86	2.77	14.3	5.5	56.0	<0.05	<0.04	<0.05	HCO3-Na
CR-1-DS	5/8/2017	22 40 56	66 08 12.1	8.23	12.7	165	87	8.1	0.13	16.7	2.90	11.8	3.16	21.3	7.08	63.7	0.01	<0.04	0.09	HCO3-Na
CR-2-DS	6/13/2013	22 40 53.9	66 07 52.9	7.19	9	311.0	n.d	n.d	0.53	15.6	1.93	12.4	3.11	12.21	7.1	73.2	<0.08	<0.2	<0.08	HCO3-Na
CR-2-DS	5/1/2015	22 40 53.9	66 07 52.9	8.94	13.6	163	61.5	n.d	0.27	16.4	2.82	12.1	3.14	15.6	6.7	62.3	<0.05	0.14	<0.05	HCO3-Na
CR-2-DS	5/8/2017	22 40 51.3	66 07 53.6	8.40	10.2	181	95	8.4	0.14	17.9	2.92	12.9	3.34	21.5	7.82	67.2	0.02	<0.04	0.12	HCO3-Na
CR-3-DS	6/13/2013	22 31 44.4	65 58 47.8	6.94	11	416.6	n.d	n.d	0.06	21.2	2.89	16.9	4.06	16.83	7.82	106.14	<0.08	1.7	<0.08	HCO3-Na
CR-3-DS	5/11/2017	22 31 44.4	65 58 47.8	8.07	10.8	315	168	9.2	almost 0	23.6	4.83	31.3	6.65	32.6	12.8	140	0.01	<0.04	0.12	HCO3-Ca
CR-4-WS	2/21/2011	22 30 56.1	66 00 39.8	7.30	22	321.9	n.d	8	n.d.	16.68	3.59	17.55	2.61	15	6	76.25	nd	n.d.	n.d.	HCO3-Ca-Na
CR-5-WS	2/21/2011	22 28 24.18	65 59 40.22	7.50	16.5	169.7	n.d	6.8	n.d.	12.76	2.69	9.4	1.9	9	5	38.43	nd	n.d.	n.d.	HCO3-Na
CR-5-DS	6/14/2013	22 28 24.18	65 59 40.22	9.03	12.8	316.6	n.d	n.d	0.25	27.7	5.09	27	6.37	40.91	15.08	113.521	1.16	<0.2	<0.08	HCO3-Na
CR-5-DS	5/4/2015	22 28 24.18	65 59 40.22	8.52	5.8	290.3	110	n.d	0.12	24.8	4.29	25.2	6.12	39.9	13.2	92.3	2.96	<0.04	<0.05	HCO3-Ca-Na
CR-5-DS	12/6/2016	22 28 24.18	65 59 40.22	9.20	25.4	253	133	8.8	almost 0	23.2	5.13	20.2	4.53	28.5	10.3	92.6	1.08	<0.04	0.14	HCO3-Na
CR-5-DS	5/12/2017	22 28 24.18	65 59 40.22	8.26	9.1	210	110	7.9	0.08	23.1	4.76	20.5	4.64	30.1	12.8	92.9	2.57	<0.04	0.18	HCO3-Na
CR-6-DS	6/14/2013	22 26 11.7	65 58 46.9	8.57	12.4	338.3	n.d	n.d	0.26	29.4	5.33	28.6	6.9	41.63	15.69	124.44	1.21	1.43	0.23	HCO3-Na-Ca
CR-7-DS	6/14/2013	22 24 46.1	65 58 35.85	8.67	8.2	352.4	n.d	n.d	n.d.	30.3	5.73	29.5	7.31	45.05	17.92	126.08	0.57	1.98	<0.08	HCO3-Na-Ca
CR-7-DS	12/5/2016	22 24 43.1	65 58 39.7	9.52	28.6	267	140	n.d	n.d.	23.9	6.03	21.0	4.57	29.9	11.1	97.9	<0.05	<0.04	0.19	HCO3-Na
CR-7-DS	5/9/2017	22 24 44	65 58 42.5	8.05	14.4	255	135	9.2	0.00	22.6	4.81	21.6	4.84	31.2	12.7	96.7	2.55	<0.04	0.19	HCO3-Na
Candado River																				
CaR-1-DS	6/13/2013	22 41 04.75	66 08 12	8.72	10.4	237.7	n.d	n.d	0.16	24.9	2.28	17.9	3.86	20.15	13.86	94.001	0.21	0.84	<0.08	HCO3-Na
CaR-1-DS	5/1/2015	22 41 04.75	66 08 12	8.54	17.3	233.1	93	n.d	0.10	23.3	3.06	18.8	4.33	21.1	12.8	85.3	<0.05	0.27	<0.05	HCO3-Na
CaR-1-DS	5/8/2017	22 41 02.4	66 08 14.5	8.70	12.3	249	131	9.1	0.02	24.6	3.23	21.5	4.37	24.6	16.5	101	0.02	<0.04	0.14	HCO3-Na
Santa Catalina River																				
SCatR-1-DS	5/10/2017	21 57 22.7	66 03 21.6	7.24	10	227	120	9.6	0.10	16.1	2.48	16.7	7.38	48.6	14.7	48.1	0.02	<0.04	0.12	SO4-Ca-Na
SCatR-2-DS	5/10/2017	21 55 50.7	66 03 10.8	8.42	13.8	227	115	10.6	0.21	16.1	2.43	15.8	6.69	47.3	14.4	45.3	0.01	<0.04	0.13	SO4-Na-Ca
SCatR-3-DS	12/6/2016	22 17 25.4	65 59 15	8.40	21.9	412	218	6	almost 0	25.1	4.88	31.7	10.0	101	21.5	47.4	5.53	0.22	0.16	SO4-Ca
SCatR-3-DS	5/12/2017	22 17 25.4	65 59 15	7.65	8.9	448	236	9.8	0.00	47.6	6.13	40.7	14.2	83.2	49.7	142	0.02	<0.04	0.27	HCO3-Na
Colmayito stream																				
CoStr-DS	5/8/2017	22 39 58.1	66 11 19.6	8.14	6.9	280	146	8	x	17.7	4.63	25.4	5.71	57.4	11.5	66.9	0.03	<0.04	0.15	HCO3-Ca
Chajarahuaico River																				
ChR-DS	5/8/2017	22 40 28.2	66 11 10.8	7.25	14.8	139	73	8.6	0.13	15.9	2.37	9.22	2.63	12.1	5.64	64.1	0.01	<0.04	0.07	HCO3-Na
Lopiara River																				
LopR-DS	5/8/2017	22 40 17.1	66 10 40.4	7.53	16.4	208	110	8.6	0.04	17.7	3.20	15.2	4.88	44.2	7.84	51.9	0.21	<0.04	0.14	HCO3-Na
Colquimayo River																				
ColR-DS	5/11/2017	22 31 40.8	66 12 7.5	8.23	12.3	271	143	10.2	0.05	33.6	2.98	16.7	6.97	40.1	16	123	0.01	<0.04	0.17	HCO3-Na
Guayatayoc River																				
G-DS	5/12/2017	22 16 06.7	66 02 01.0	7.61	7.5	242	127	10.6	0.10	15.9	1.68	15.9	14.0	90.7	12.7	28.0	0.01	<0.04	0.16	SO4-Ca-Na
Peñas Blancas River																				
PBR-1-WS	3/27/2012	22 35 32.3	66 03 30.8	8.71	21.3	325.5	n.d	7.5	n.d.	29.2	6.07	22.2	4.71	27.2	28.9	124.44	<0.01	0.1	0.22	HCO3-Na
PBR-2-WS	3/27/2012	22 35 25.65	66 3 24.31	8.36	15.5	297.1	n.d	n.d	n.d.	32.3	6.32	24	5.29	29.7	31.9	120	<0.01	0.1	0.15	HCO3-Na
Los Pozuelos Lagoon																				
PL-1-DS	6/14/2013	22 24 49.4	65 58 48.1	7.03	15	1589.7	n.d	n.d	x	236	24.8	54	17	145.37	308.09	175.68	<0.08	<0.2	<0.08	Cl-Na
PL-1-DS	12/14/2016	22 23 55.6	65 59 54.5	7.98	25.2	365	190	8.2	x	33.5	8.63	24.9	5.41	40.9	19.3	116	<0.05	0.22	0.19	HCO3-Na
PL-1-DS	5/9/2017	22 24 53.4	65 59 37.4	9.74	14.4	344	182	10.1	x	40.9	9.30	23.0	2.84	70.0	24.1	74.1	0.07	<0.04	0.38	HCO3-Na
PL-2-DS	5/3/2015	22 24 49.4	65 58 48.1	8.68	15.5	5660	n.d	n.d	x	990	97.2	113	53.4	594.8	1353.1	337.8	<0.05	2.13	4.0	Cl-Na
PL-2-DS	12/5/2016	22 24 56.3	65 59 20.6	9.69	18.9	288	150	n.d	x	29.1	7.25	21.8	3.69	35.7	14.5	96	<0.05	0.22	0.21	HCO3-Na
PL-3-DS	5/3/2015	22 24 40.5	66 00 57.1	8.71	15.7	5460	n.d	n.d	x	988	95	112	52.9	536.7	1346.0	311.7	<0.05	1.28	4.2	Cl-Na

TDS = Total dissolved solids

DO = Dissolved oxygen

Table 2. Surface water samples, arsenic and iron content and speciation.

`		As(T)	As(III)	As(V)	Fe(T)	Fe(II)	Fe(III)
SAMPLE	**DATE**	**µg/L**	**µg/L**	**µg/L**	**µg/L**	**µg/L**	**µg/L**
Cincel River							
CR-1-DS	6/13/2013	4.57	n.d.	n.d.	<100	n.d.	n.d.
CR-1-DS	5/1/2015	3.5	<1	3.5	9.5	7.8	1.7
CR-1-DS	5/8/2017	7.33	1.9	5.43	10	8	2
CR-2-DS	6/13/2013	5.55	n.d.	n.d.	<100	n.d.	n.d.
CR-2-DS	5/1/2015	4.8	<1	4.8	6.9	6.5	0.4
CR-2-DS	5/8/2017	7.58	0.5	7.08	6	6	0
CR-3-DS	6/13/2013	7.49	n.d.	n.d.	<100	n.d.	n.d.
CR-3-DS	5/11/2017	12.1	0.3	11.8	11	11	0
CR-4-WS	2/21/2011	5.13	n.d.	n.d.	30	n.d.	n.d.
CR-5-DS	6/14/2013	13.9	n.d.	n.d.	<100	n.d.	n.d.
CR-5-WS	2/21/2011	7.03	n.d.	n.d.	10	n.d.	n.d.
CR-5-DS	5/12/2017	16	0	16	15	15	0
CR-5-DS	12/6/2016	20.2	0.9	19.3	18	18	0
CR-5-DS	5/4/2015	1.8	<1	1.8	9.7	9.3	0.5
CR-6-DS	6/14/2013	15.1	n.d.	n.d.	<100	n.d.	n.d.
CR-7-DS	6/14/2013	17.8	n.d.	n.d.	<100	n.d.	n.d.
CR-7-DS	5/9/2017	18.5	0.5	18	9	7	2
CR-7-DS	12/5/2016	20.3	1.3	19	32	31	1
Candado River							
CaR-1-DS	6/13/2013	11.3	n.d.	n.d.	<100	n.d.	n.d.
CaR-1-DS	5/1/2015	7.9	7.9	0.0	7.4	7.1	0.4
CaR-1-DS	5/8/2017	17	0.3	16.7	5	5	0
Santa catalina River							
SCatR-1-DS	5/10/2017	1.81	<0.3	1.81	19	19	0
SCatR-2-DS	5/10/2017	1.46	<0.3	1.46	23	<2	23
SCatR-3-DS	12/6/2016	<1	n.d.	n.d.	117	0	117
SCatR-3-DS	5/12/2017	2.09	1.9	0.19	10	10	0
Colmayito Stream							
CoStr-DS	5/8/2017	5.03	0.6	4.43	23	19	4
Chajarahuaico River							
ChR-DS	5/8/2017	6.21	0.3	5.91	15	15	0
Lopiara River							
LopR-DS	5/8/2017	4.29	<0.3	4.29	12	12	0
Colquimayo River							
ColR-DS	5/11/2017	6.47	<0.3	6.47	13	13	0
Guayatayoc River							
GR-DS	5/12/2017	1.61	<0.3	1.61	94	53	41
Peñas Blancas River							
PBR-1-WS	3/27/2012	22.8	n.d.	n.d.	210	n.d.	n.d.
PBR-2-WS	3/27/2012	27	n.d.	n.d.	90	n.d.	n.d.
Los Pozuelos Lagoon							
PL-1-DS	6/14/2013	47.5	n.d.	n.d.	<100	n.d.	n.d.
PL-1-DS	12/14/2016	45.2	1.9	43.3	26	26	0
PL-1-DS	5/9/2017	56.5	3.7	52.8	21	21	0
PL-2-DS	5/3/2015	200.3	89.5	110.8	111.8	109.6	2.2
PL-2-DS	12/5/2016	43.7	2.2	41.5	215	210	5
PL-3-DS	5/3/2015	149.4	133.7	15.7	133.9	128.7	5.2

n.d. = not determined

Table 3. Groundwater samples, field parameters and major ions.

SAMPLE	Sampling date	Lat	Long	pH	T	Cond.	TDS	DO	Depth	Na	K	Ca	Mg	SO4	Cl	HCO3	NO3	PO4	F	Water-type	Aquifer facies
		S	W		°C	µS/cm	ppm	mg/L	m	mg/L	mg/L	mg/L	mg/L	mg/L	mg/L	mg/L	mg/L	mg/L	mg/L		
W1-DS	6/14/2013	22 40 04.4	66 08 19.8	6.98	n.d.	612	n.d.	n.d.	1.6	74.7	11.1	42.7	11.4	78.3	34.8	190.3	2.6	2.17	<0.08	HCO3-Na	AD
W2-WS	3/28/2012	22 37 59.6	66 03 01.1	6.94	n.d.	348	235	2.2	0.2	27.8	5.1	29.0	9.0	44.6	17.8	98.8	0.5	0.06	0.07	HCO3-Ca	AD
W2-DS	6/13/2013	22 37 59.6	66 03 01.1	7.81	7.1	310	248	n.d.	1.1	25.5	4.3	27.5	8.1	32.4	17.9	102.5	<0.08	2.59	<0.08	HCO3-Ca	AD
W4-DS	6/14/2013	22 33 53.2	66 01 18.9	8.38	10.7	631	316	n.d.	1.8	39.6	6.6	60.6	21.0	121.3	36.1	106.1	35.3	1.48	<0.08	SO4-Ca	AD
W5-DS	6/14/2013	22 33 32.0	66 1 30.49	6.89	n.d.	624	n.d.	n.d.	2.2	27.4	4.5	59.0	22.6	46.8	79.5	87.8	45.4	2.9	0.23	HCO3-Ca	AD
W5-DS	5/3/2015	22 33 32.0	66 1 30.49	6.7	13.4	510	255	n.d.	1.9	23.3	4.2	50.4	17.3	52.0	51.1	89.6	50.5	1.88	0.54	HCO3-Ca	AD
W5-DS	5/12/2017	22 33 32.0	66 1 30.49	7.58	12.7	744	393	4.2	3.0	29.0	5.9	70.9	25.7	66.6	97.4	87.2	98.9	1.16	0.28	HCO3-Ca	AD
W7-DS	6/16/2013	22 32 20.5	65 57 41.9	7.02	n.d.	233	n.d.	n.d.	n.d.	8.7	4.0	27.9	7.9	17.1	9.6	84.2	3.0	1.29	<0.08	HCO3-Ca	AD
W12-DS	5/12/2017	22 29 59.9	66 02 39.6	7.96	11.8	131	69	7.3	3.4	10.7	2.7	13.5	3.4	18.0	7.3	47.1	10.9	<0.04	0.23	HCO3-Ca	AD
W13-DS	12/6/2016	22 27 51.4	66 04 24.3	8.46	17.7	204	108	n.d.	7.5	12.2	1.7	18.5	5.2	26.9	9.8	56.3	10.1	0.20	0.06	HCO3-Ca	AD
W13-DS	5/9/2017	22 27 51.4	66 04 24.1	7.48	13.2	197	104	6.5	7.4	13.1	1.7	16.8	5.1	26.9	9.5	58.2	8.4	0.26	0.11	HCO3-Ca	AD
W15-DS	5/10/2017	22 17 46.4	65 54 59.3	7.26	12.3	645	343	n.d.	n.d.	58.8	5.3	57.5	14.9	142.0	26.8	185.0	8.0	<0.04	0.17	HCO3-Ca	AD
W16-DS	5/10/2017	22 02 56.9	65 55 04.3	7.7	14.2	156	84	6.9	2.5	9.6	2.3	12.5	5.0	19.9	6.2	49.9	7.0	0.31	0.09	HCO3-Ca	AD
W6-WS	2/21/2011	22 31 08.7	66 00 47.2	7.9	15.1	867	318	4.3	2.5	45.5	32.1	81.7	20.7	104.6	123.9	127.5	n.d.	n.d.	< 0.3	HCO3-Ca	LS
W6-DS	6/14/2013	22 31 08.7	66 00 47.2	7.53	n.d.	737	n.d.	n.d.	2.1	35.3	18.0	83.4	17.3	102.4	63.7	157.4	22.4	0.93	0.21	HCO3-Ca	LS
W6-DS	5/3/2015	22 31 08.7	66 00 47.2	7.63	16.6	977	489	n.d.	2.2	49.6	50.9	93.4	21.1	83.3	75.3	234.1	119.5	1.89	0.15	HCO3-Ca	LS
W8-WS	2/21/2011	22 30 23.2	65 59 46.8	7.9	15.8	1141	584	2.9	2.0	62.1	70.6	101.6	26.1	114.4	163.5	178.0	n.d.	n.d.	n.d.	HCO3-Ca	LS
W8-DS	6/14/2013	22 30 23.2	65 59 46.8	6.84	n.d.	252	n.d.	n.d.	1.0	6.1	44.1	12.7	3.8	23.1	5.0	73.2	13.1	8.16	<0.08	HCO3-K	LS
W8-DS	5/3/2015	22 30 23.2	65 59 46.8	7.78	14.6	288	144	n.d.	1.5	7.3	48.9	12.7	4.2	23.9	5.1	78.6	25.1	10.88	<0.05	HCO3-K	LS
W9-WS	2/21/2011	22 28 23.2	65 59 37.4	7.3	13.9	969	438	2.7	n.d.	93.3	9.4	76.1	19.3	172.1	104.1	178.1	n.d.	n.d.	< 0.3	HCO3-Na	LS
W9-DS	6/14/2013	22 28 23.2	65 59 37.4	7.45	n.d.	1355	n.d.	n.d.	1.9	112.0	11.8	144.0	29.4	399.5	119.5	120.8	3.6	<0.2	<0.08	SO4-Na	LS
W9-DS	5/2/2015	22 28 23.2	65 59 37.4	7.12	12.9	843	422	n.d.	n.d.	81.7	9.6	78.2	16.0	223.7	40.2	171.2	5.8	<0.04	<0.05	SO4-Na	LS
W9-DS	12/6/2016	22 28 23.2	65 59 37.4	7.95	14.6	650	342	n.d.	2.0	61.4	7.0	42.5	8.5	128.0	19.4	147.0	6.8	<0.04	0.22	HCO3-Na	LS
W9-DS	5/11/2017	22 28 23.2	65 59 37.4	7.65	11.6	478	254	4.8	2.1	56.7	6.3	32.8	7.0	91.5	15.4	151.0	7.6	<0.04	0.32	HCO3-Na	LS
W11-DS	5/12/2017	22 30 12.6	66 01 49.1	7.79	10.1	213	113	5.4	1.8	12.6	4.1	23.5	4.4	20.3	8.7	91.0	4.0	0.93	0.24	HCO3-Ca	LS
W14-DS	12/14/2016	22 27 54.2	66 0 41.6	8.05	14.9	213	109	7.1	2.0	18.7	7.6	13.7	2.8	16.6	11.9	69.9	5.7	0.28	0.14	HCO3-Na	LS
W14-DS	5/9/2017	22 27 54.5	66 0 41.3	7.78	10.1	189	99	5.3	0.9	19.3	7.7	11.4	2.9	15.4	12.2	68.3	5.6	<0.04	0.22	HCO3-Na	LS
W3-DS	6/13/2013	22 36 17	66 04 10	7.61	11.8	251	191	3.4	n.d.	16.1	3.8	28.9	4.5	22.7	8.1	91.5	7.7	<0.2	<0.08	HCO3-Ca	VR
CAA														400	350				0.9-1.7		
WHO														500					1.5		

TDS = Total dissolved solids

DO = Dissolved oxygen

AD = aluvial deposits

LS = lacustrine sediments

VR = volcanic rocks

CAA = Código Alimetario Argentino, 2012

WHO = World Health Organization, 2017

n.d. = not determined

Table 4. Groundwater samples, arsenic and iron content

SAMPLE	Sampling date	As (T)	As (III)	As(V)	Fe (T)	Fe(II)	Fe(III)	Aquifer facies
		µg/L	µg/L	µg/L	µg/L	µg/L	µg/L	
W1-DS	6/14/2013	16.1	n.d.	n.d.	<100	n.d.	n.d.	AD
W2-WS	3/28/2012	10.8	n.d.	n.d.	100	n.d.	n.d.	AD
W2-DS	6/13/2013	8.9	n.d.	n.d.	110	n.d.	n.d.	AD
W4-DS	6/14/2013	21.4	n.d.	n.d.	<100	n.d.	n.d.	AD
W5-DS	6/14/2013	29.7	n.d.	n.d.	<100	n.d.	n.d.	AD
W5-DS	5/3/2015	18.4	<1	18.4	3	2	1	AD
W5-DS	5/12/2017	23.1	0.5	22.6	2	2	0	AD
W7-DS	6/16/2013	14.1	n.d.	n.d.	240	n.d.	n.d.	AD
W12-DS	5/12/2017	8.21	2.5	5.71	9	9	0	AD
W13-DS	12/6/2016	5.2	<0.8	5.2	<2	<2	0	AD
W13-DS	5/9/2017	6.33	<0.3	6.33	12	7	5	AD
W15-DS	5/10/2017	5.67	<0.3	5.67	13	2	11	AD
W16-DS	5/10/2017	3.82	0.4	3.42	32	15	17	AD
W6-WS	2/21/2011	55	n.d.	n.d.	<10	n.d.	n.d.	LS
W6-DS	6/14/2013	54.7	n.d.	n.d.	<100	n.d.	n.d.	LS
W6-DS	5/3/2015	69.0	0.9	68.0	<2	<2	0	LS
W8-WS	2/21/2011	74.3	n.d.	n.d.	<10	n.d.	n.d.	LS
W8-DS	6/14/2013	113	n.d.	n.d.	<100	n.d.	n.d.	LS
W8-DS	5/3/2015	90.2	1.1	89.1	1290	259	1031	LS
W9-WS	2/21/2011	19.9	n.d.	n.d.	<10	n.d.	n.d.	LS
W9-DS	6/14/2013	16.1	n.d.	n.d.	<100	n.d.	n.d.	LS
W9-DS	5/2/2015	10.0	<1	10.0	8	7	1	LS
W9-DS	12/6/2016	19.1	<0.8	19.1	3	2	1	LS
W9-DS	5/11/2017	19.6	0.6	19	13	9	4	LS
W11-DS	5/12/2017	33.6	0.7	32.9	5	5	0	LS
W14-DS	12/14/2016	12.4	<0.8	12.4	2	2	0	LS
W14-DS	5/9/2017	12.3	<0.3	12.3	5	5	0	LS
W3-DS	6/13/2013	8.2	n.d.	n.d.	<100	n.d.	n.d.	VR
CAA		50						
WHO		10						

AD = aluvial deposits

LS = lacustrine sediments

VR = volcanic rocks

CAA = Código Alimetario Argentino, 2012

WHO = World Health Organization, 2017

n.d. = not determined

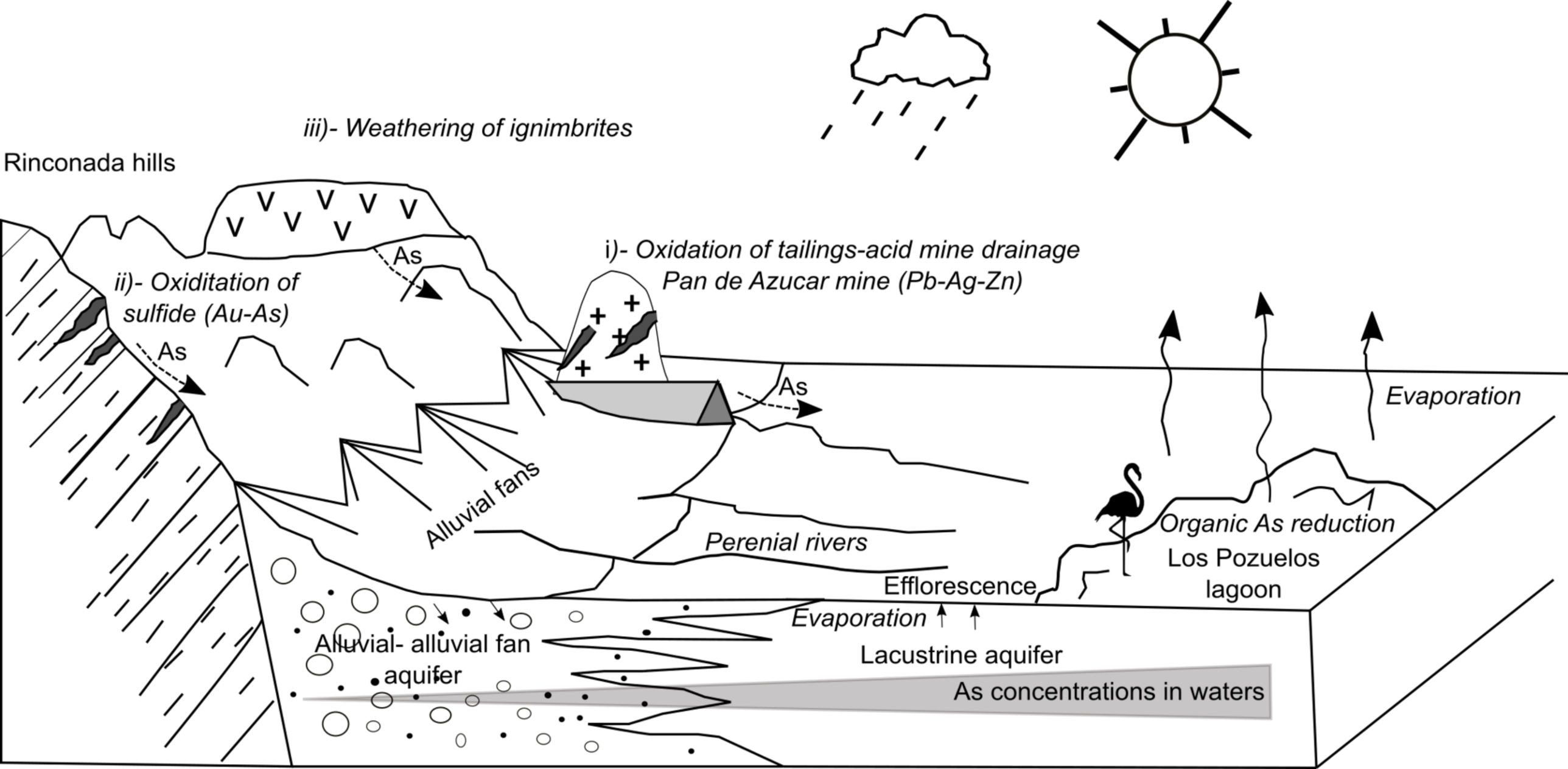
iii)- Weathering of ignimbrites
Rinconada hills
ii)- Oxiditation of
sulfide (Au-As)
As
As
i)- Oxidation of tailings-acid mine drainage
Pan de Azucar mine (Pb-Ag-Zn)
As
Evaporation
Alluvial fans
Perenial rivers
Organic As reduction
Los Pozuelos
lagoon
Efflorescence
Evaporation
Alluvial- alluvial fan
aquifer
Lacustrine aquifer
As concentrations in waters